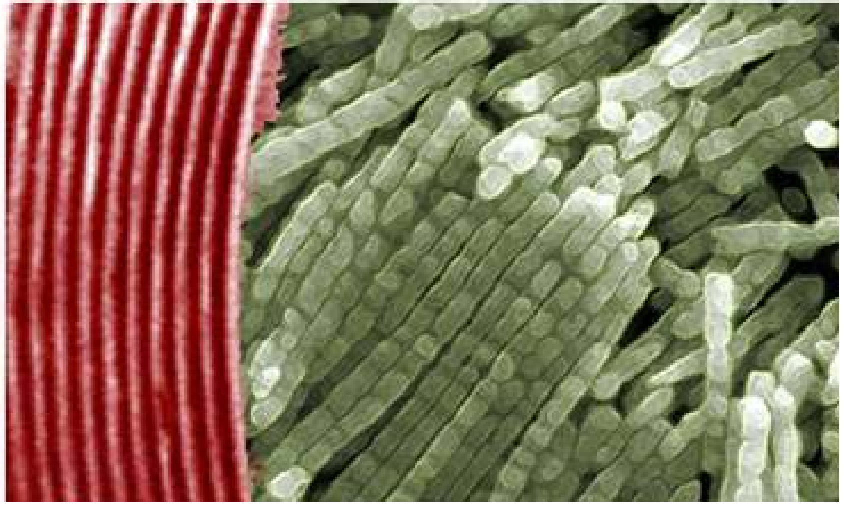

Thermoelectric Nanostructures: From Chemical Synthesis towards Physical Model Systems

Prof. Dr. Kornelius Nielsch
Institute of Applied Physics, University of Hamburg, Germany

Potential Applications of TE Generator

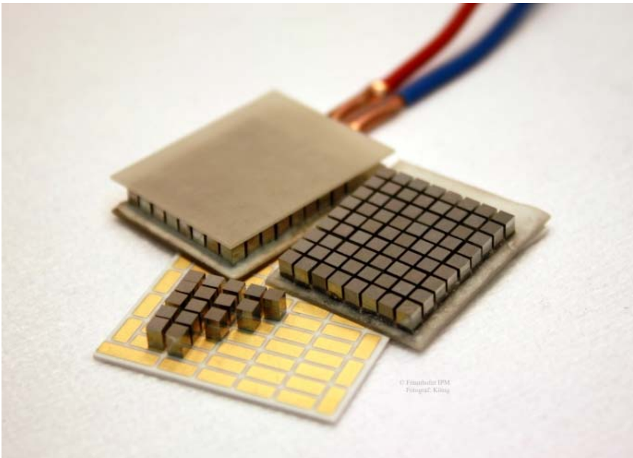

High-T TE Generators in Heating Systems

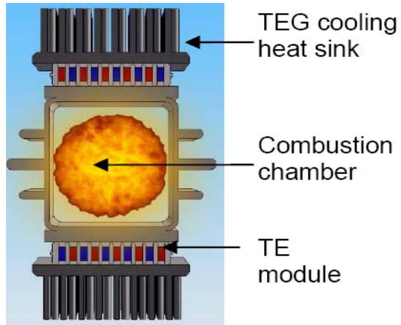

Heat Recovery in Industry

Heat Recovery in Cars

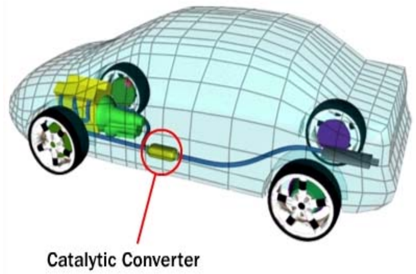

Wireless Sensors

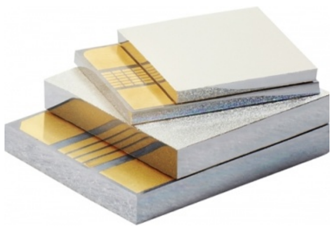

Thermoelectric Efficiency: ZT

$$ZT = \frac{S^2 \sigma}{\kappa} T \sim 0{,}5\text{-}1$$

High Output Potentials: Seebeck coefficient

Low Thermal Conductivity

High Electric Conductivity

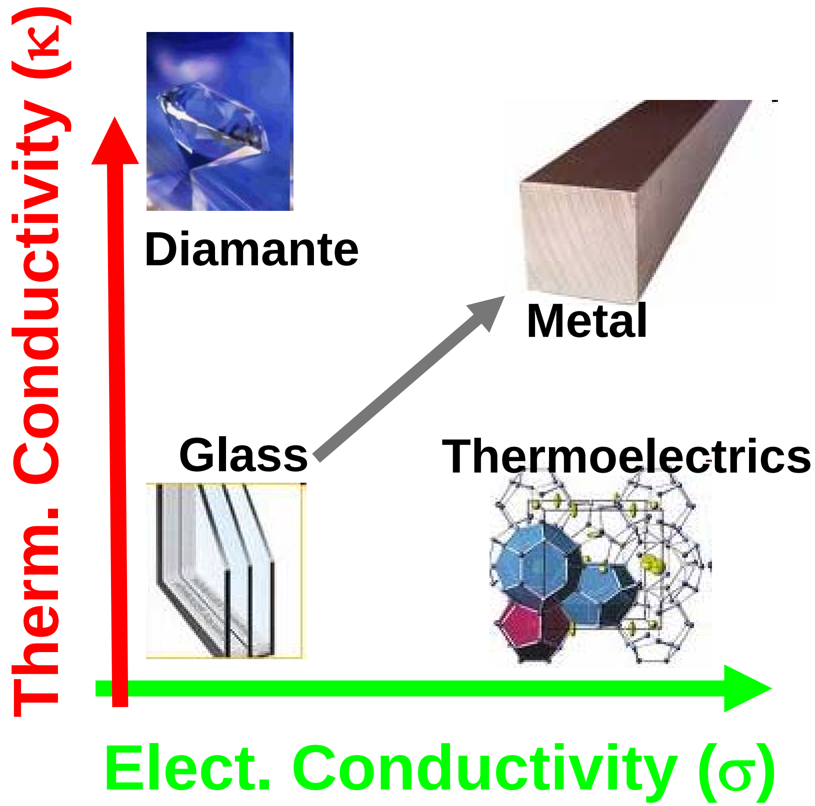

Important Thermoelectric Materials

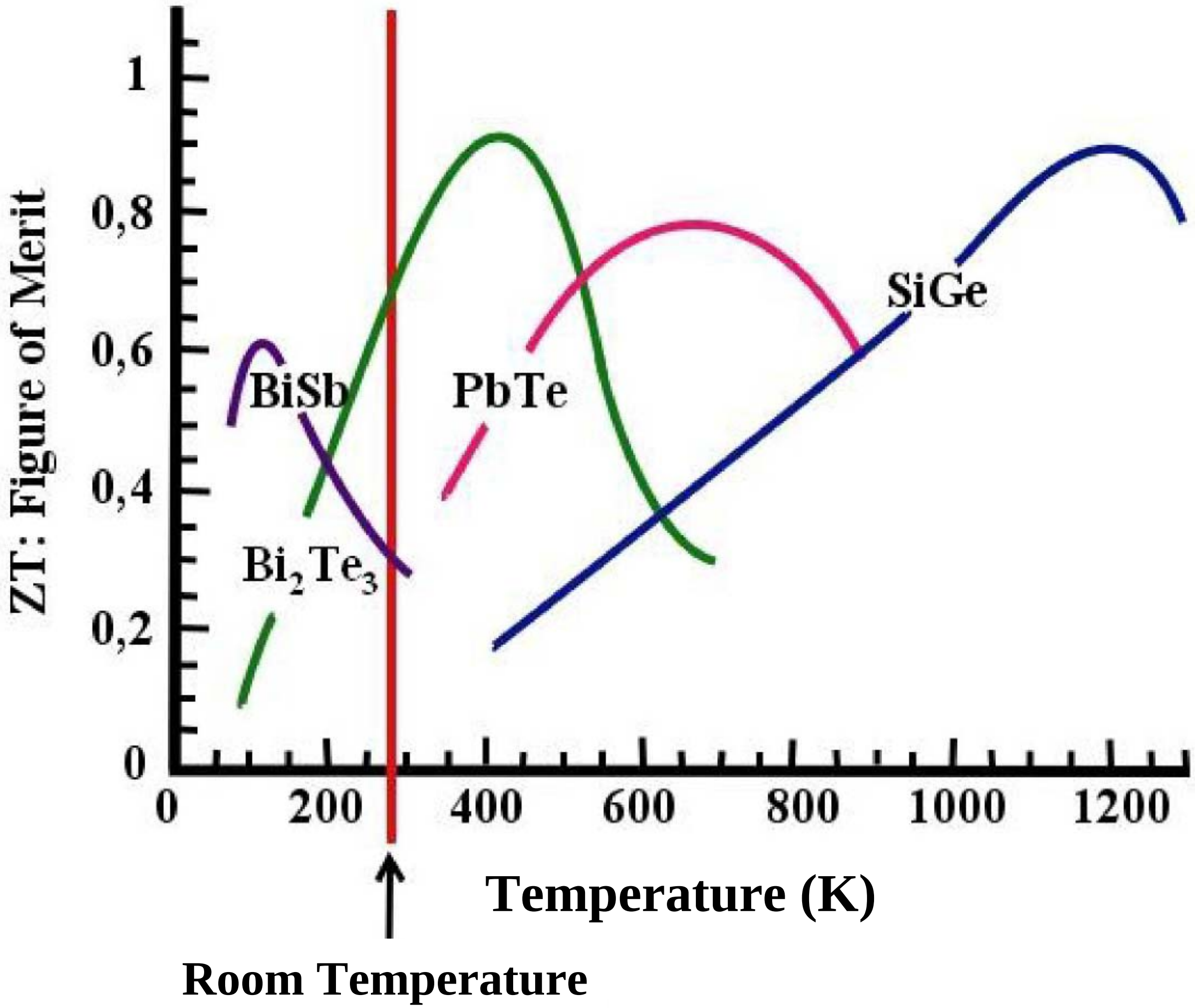

Overview of Thermoeletric Materials

High-temperatures materials

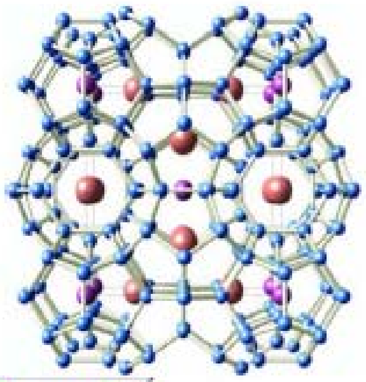

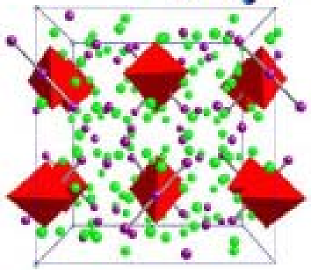

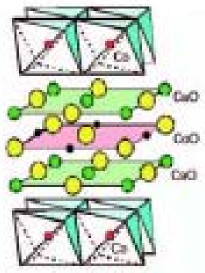

$Ca_3Co_4O_9$

• PbTe	(Pb,Sn)Te, PbTe-$AgSbTe_2$
• TAGS	Te-Ag-Ge-Sb
• Zn_4Sb_3	
• Silicides	p-$MnSi_{1.73}$, n-$Mg_2Si_{0.4}Sn_{0.6}$,
• Si/Ge	$Si_{0.80}Ge_{0.20}$
• n/p-Skutterutide	$CoSb_3$
• n/p-Half Heusler	$(Ti_{0,5}(Zr_{0,5}Hf_{0,5})_{0,5})NiSn_{1-y}Sb_y$ TiNiSn
• n/p-Clathrates	$Ba_8Ga_{16}Ge_{30}$
• Oxides	p-$NaCo_2O_4$
• Zintl Phases	p-$Yb_{14}MnSb_{11}$
• Th_3P_4	$La_{3-x}Te_4$

Thermoelectric Materials of the 20th Century

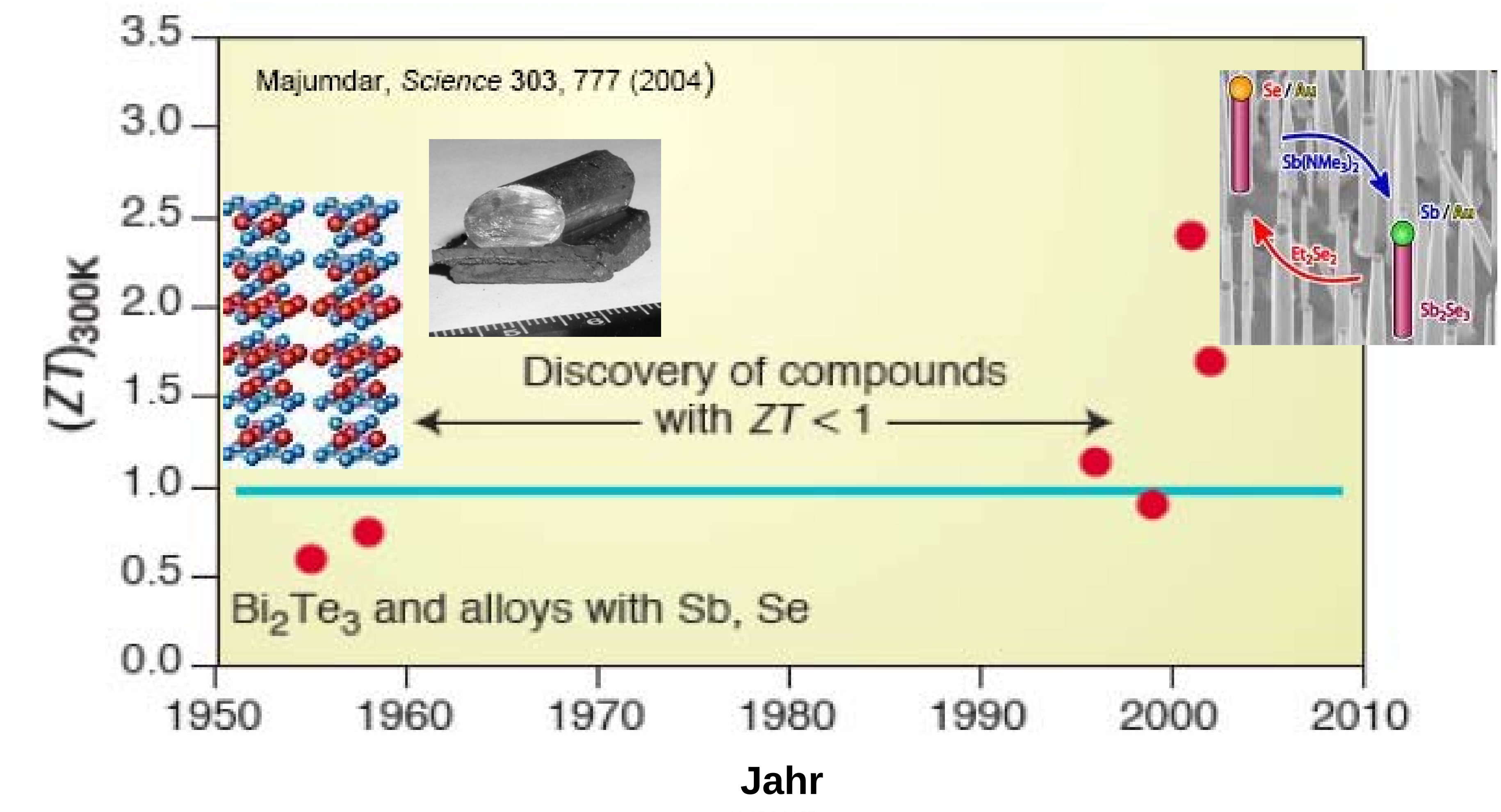

Thermoelectric Nanostructures (ZT >1)

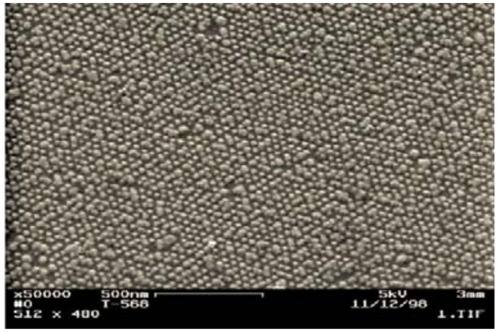

ZT~3.5 @ 575 K
quantum dot superlattice (MBE)
n-type, PbSeTe/PbTe
[Harman, MIT-LL, J. Elec.Mat. 2000]

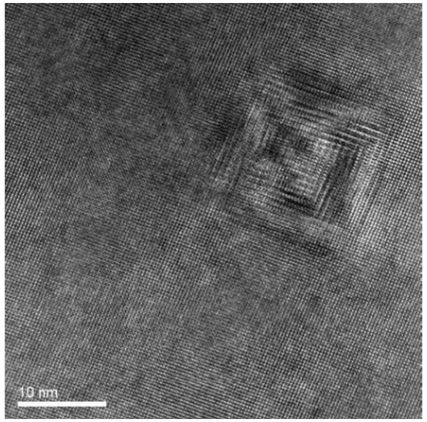

ZT~2.2 @ 800 K
bulk – 'natural' nanodots
n-type, $AgSbTe_2$-PbTe ('LAST')
[Kanatzidis, Northwestern, 2004]

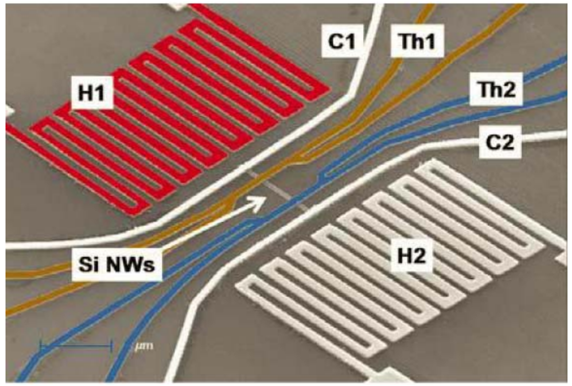

ZT~1.2 @ 350 K Nanowire p-type, Si
[Heath, Caltech, 2008]

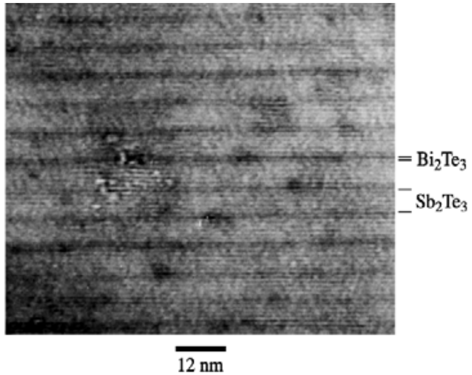

ZT~2.4 @ 300 K
superlattice (CVD)
p-type, Bi_2Te_3/Sb_2Te_3,
[Venkatasubramanian, RTI/Nextreme, 2001]

ZT~1.4 @ 373 K
bulk – fine grain
p-type, $(Bi,Sb)_2Te_3$
[15 authors, BC/MIT/GMZ Energy/Nanjing University, 2008]

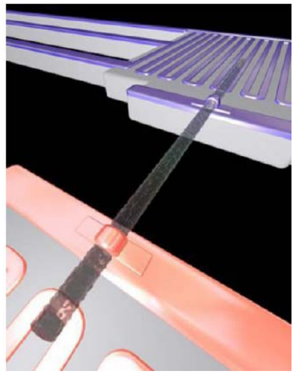

ZT~0.6 @ 300 K
nanowire
p-type, Si
[Yang/Majumdar, Berkeley, 2008]

State of the Arte for Devices: ZT < 1

Predictions for Confined Structures

Hicks and Dresselhaus, PRB 47 (1993) 12727

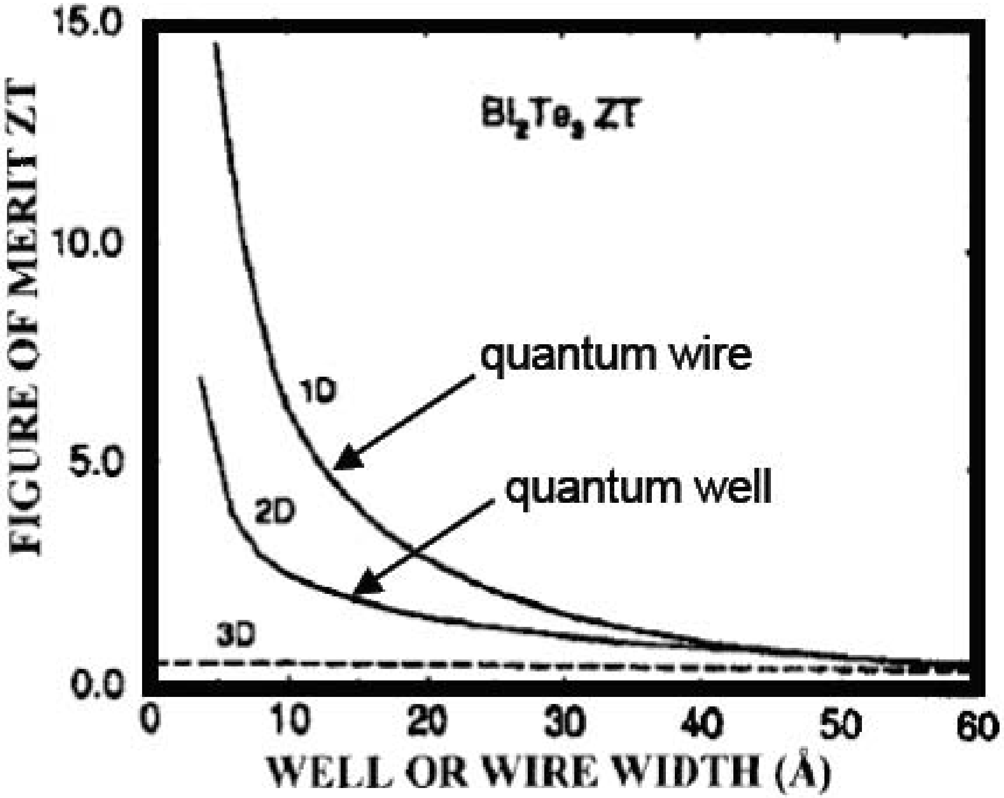

- **Does not include deleterious interface or barrier effects**
- **ZT enhanced by degeneracy: multiple carrier pockets in k-space**

ZT-Measurements of Single TE Nanowires

Material	Diameter or Cross section [nm] or [nm²]	Temperature [K]	Thermoelectric properties at 300 K σ [$10^6/(\Omega m)$]	S [µV/K]	κ [W/(mK)]	ZT	Refs.
Bi_xTe_{1-x} (sc)	81	300	0.07	-30	1.05	0.019	[T1]
Bi_xTe_{1-x} (pc) Bi_xTe_{1-x} (sc)	55 52	411 306	0.04 0.22	-90 -52	1.2 2.9	0.13 0.06	[T2]
$CrSi_2$ (sc)	78 97 103	300 300 300	0.09 0.11 0.05	+125 +120 +150	7.7 7.7 12	0.060 0.062 0.028	[T3]
Si*(sc), p-type ($7x10^{19}/cm^{-3}$)	20 x 20	200				1	[T9]

* Ensemble measurement, results were averaged over 10 to 400 nanowires.

Power Factor Calculated for n-type InSb Nanowires

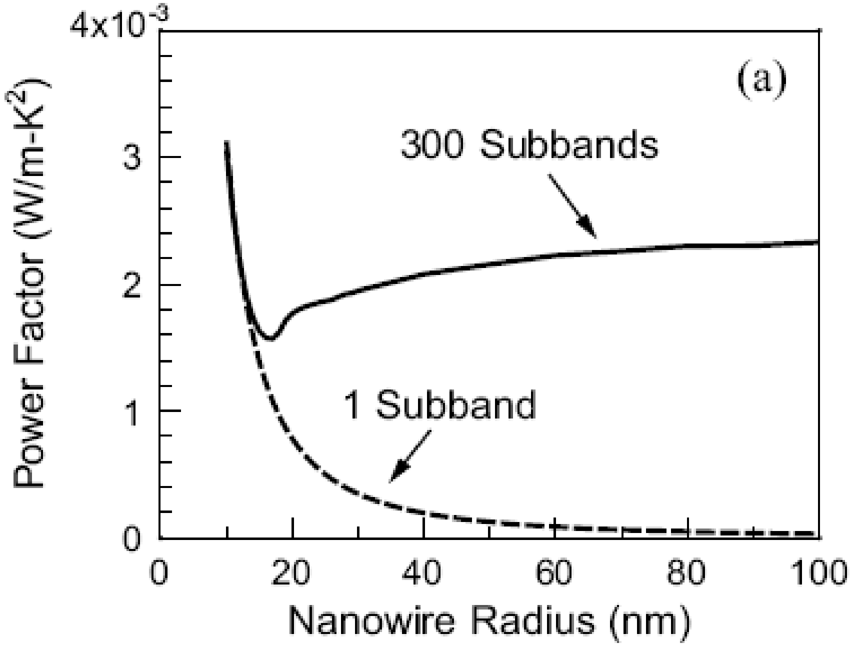

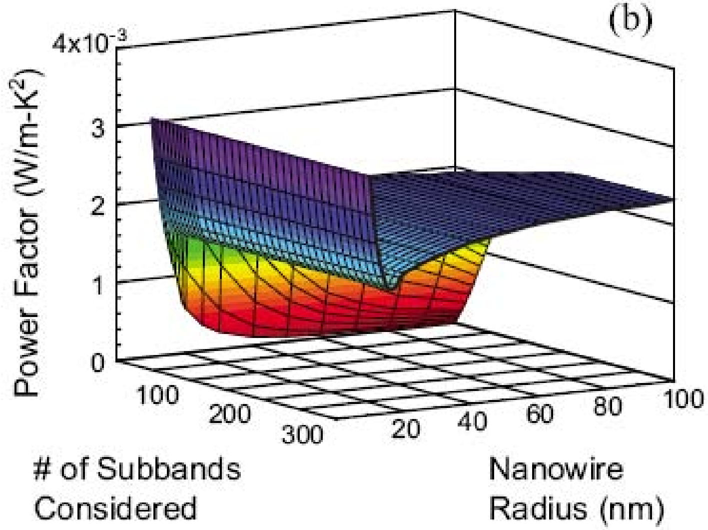

$$ZT = \frac{S^2 \sigma}{\kappa} T$$

Power Factor ($S^2\sigma$)

J.E. Cornett, O. Rabin, Appl. Lett. **98**, 182104 (2011)

Single Electron Transistor: Thermopower Measurements of InAs Nanowire with embedded Quantum Dot

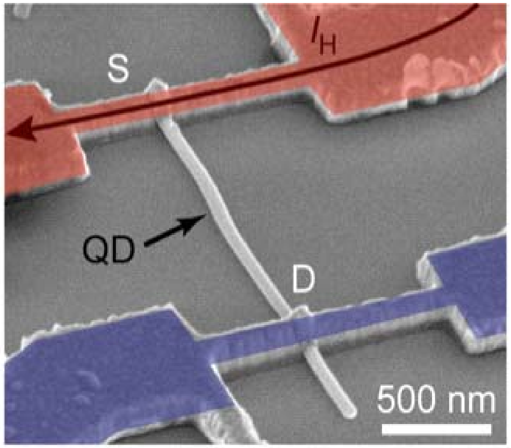

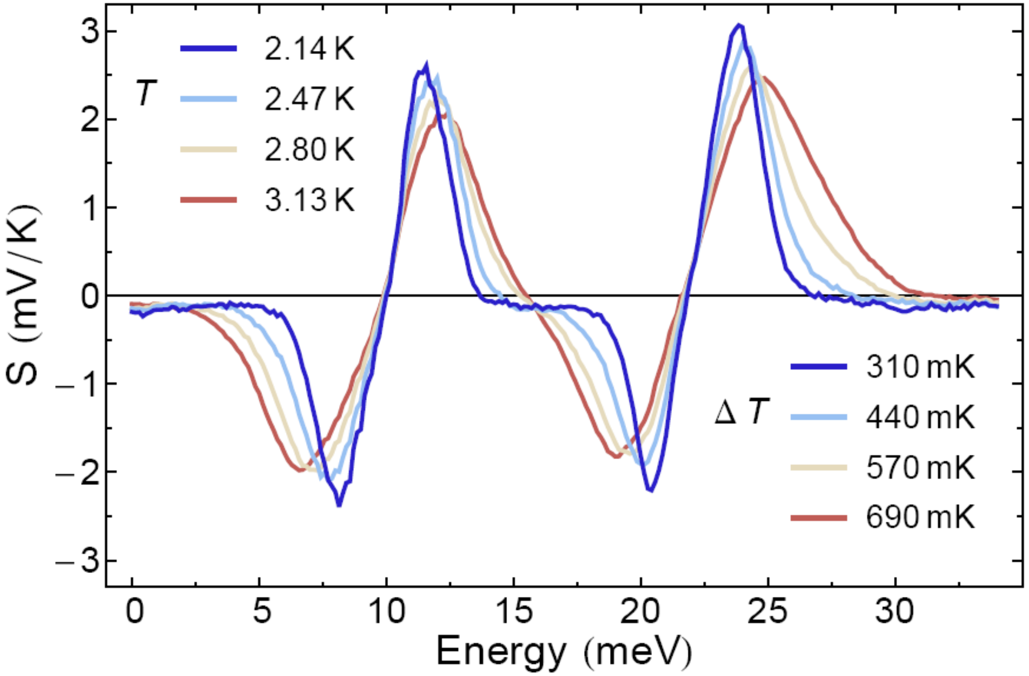

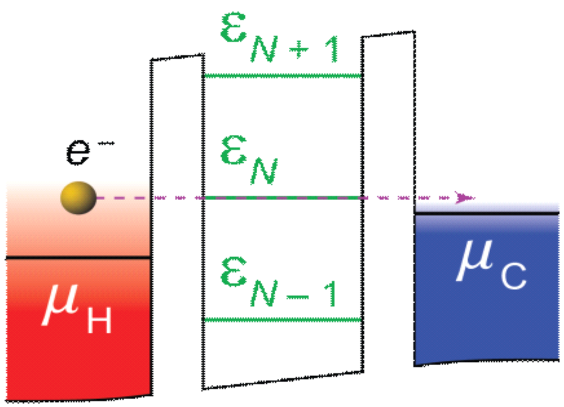

E.A. Hoffmann, H. Linke et al., *Nano Lett.* **9**, 779 (2009)

Bottom-Up: Nanowire Growth by Vapor Liquid Solid (VLS) Mode

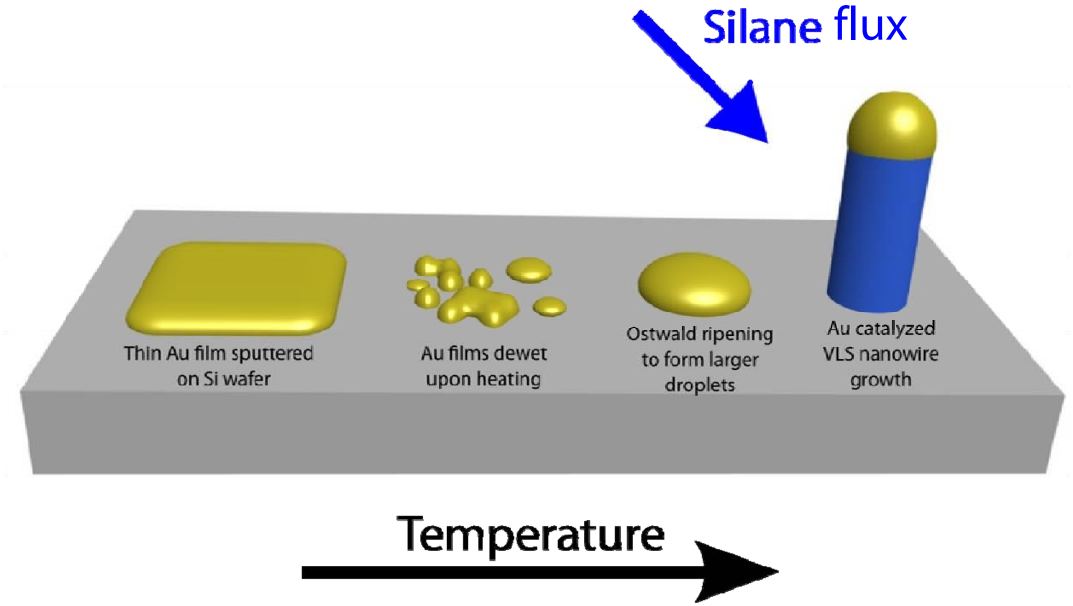

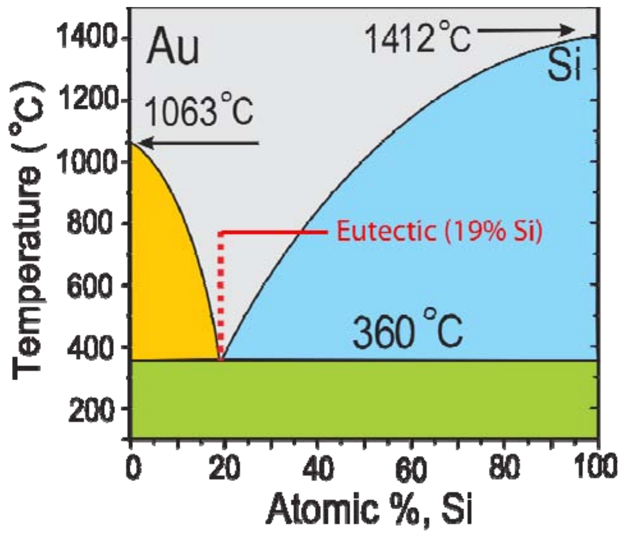

Thermal decomposition of molecular precursors (CVD) and crystallization from a catalytic droplet that defines the wire diameter.

- Nanowire growth
- Patterning possible

Top Down: Electrochemical Etched Silicon Nanowires

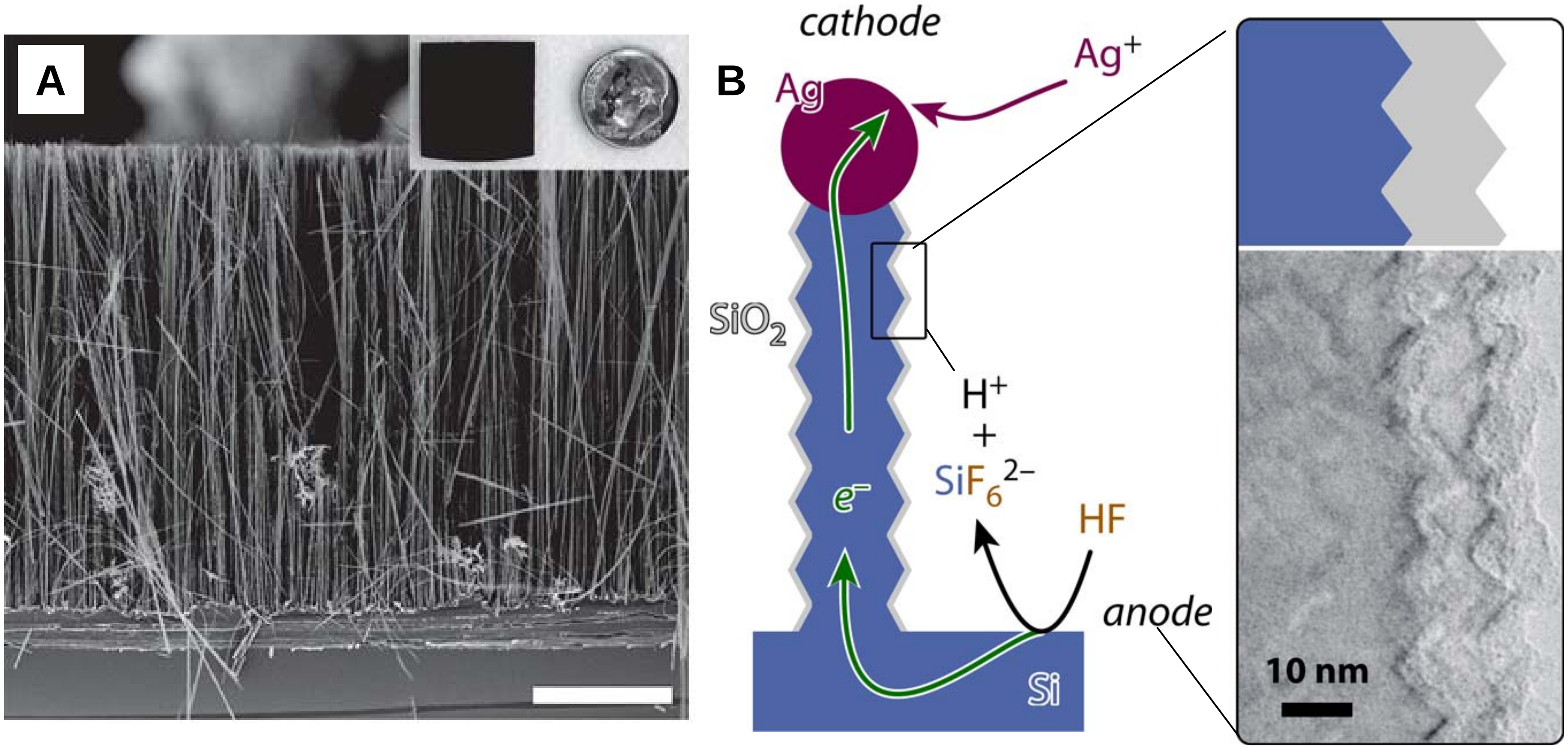

Comparison of Silicon Nanowires: Thermal Conductivity

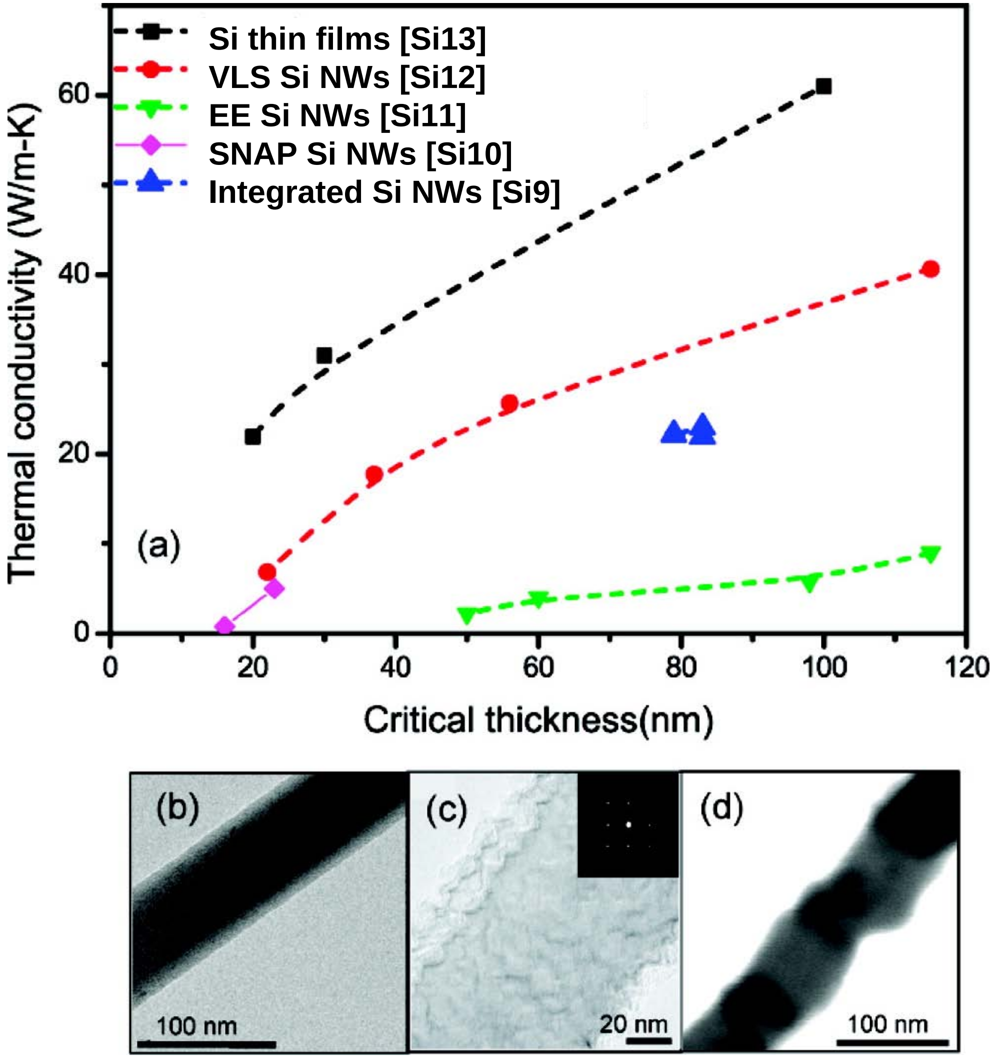

A. Majumdar et al., *Nano Lett.* **10**, 4341 (2010).

Si Nanomesh / Phononic Crystals

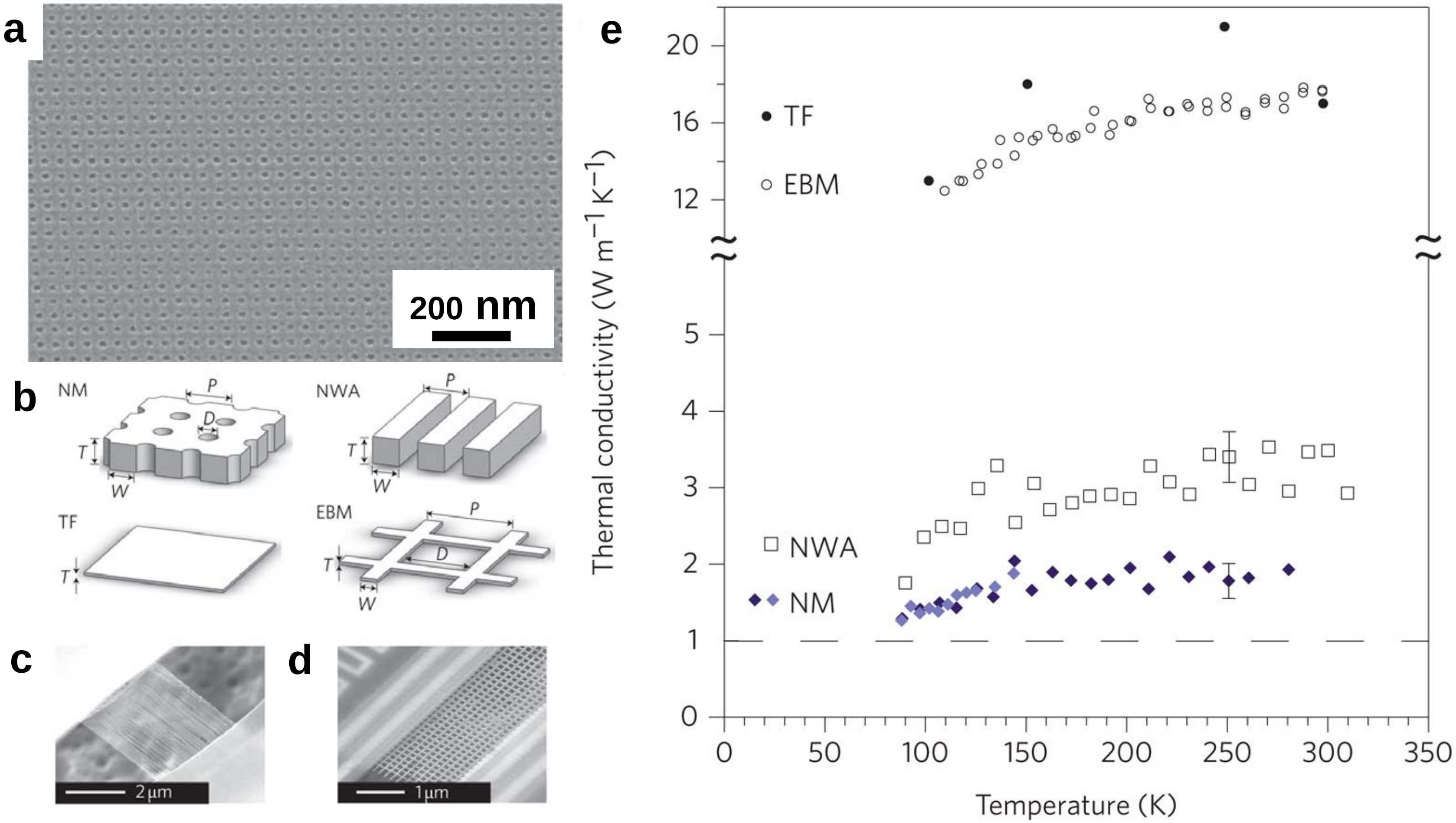

Heath et al., Nature Nanotech. 5, 718 (2010).

Thermoelectric Transport in Superlattices

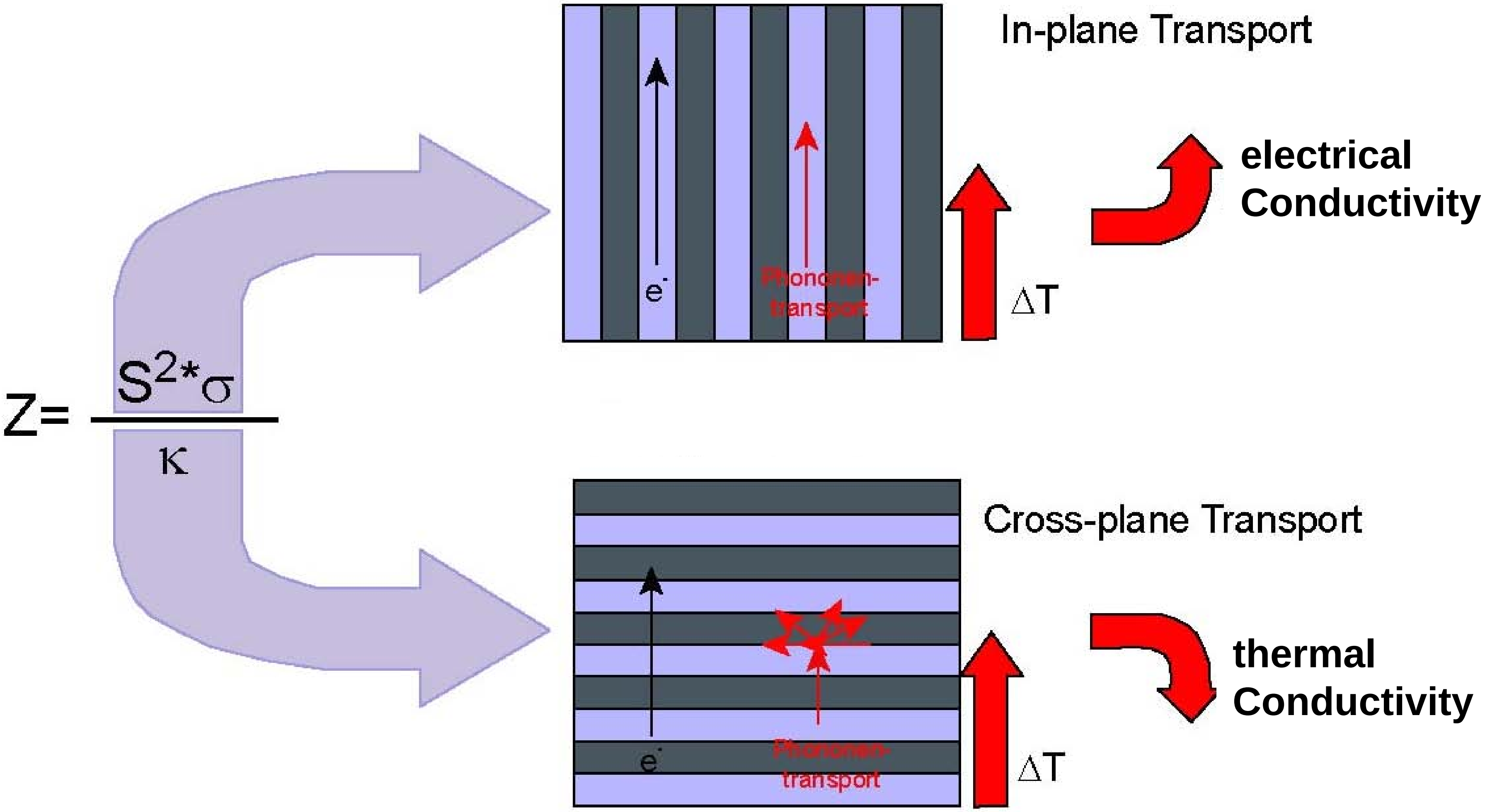

Thermal Conductivity of Ge/Si Nanodot Multilayers

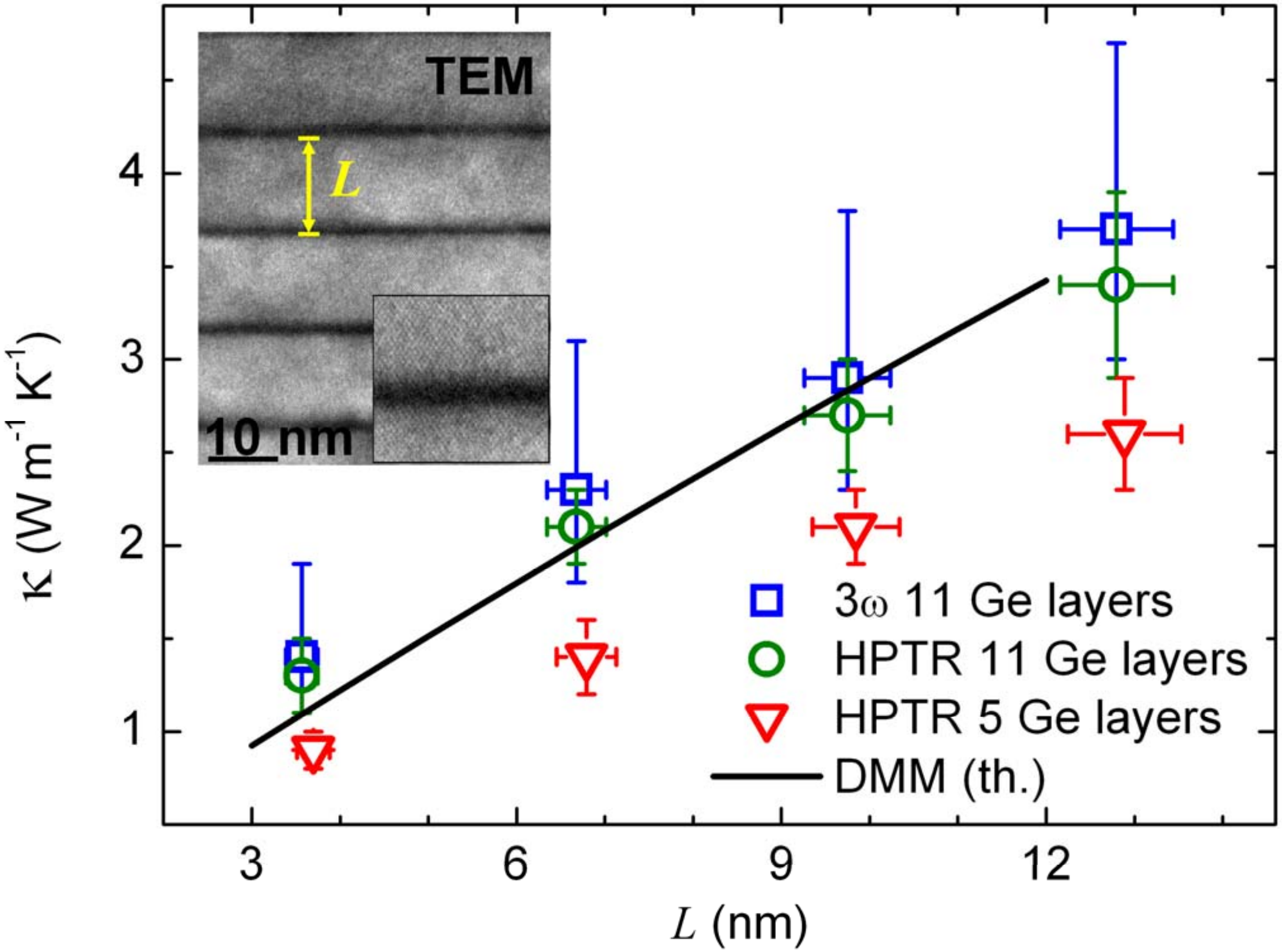

G. Pernot et al., *Nature Mater.* **9**, 491-495 (2010).

Thermionic Superlattice

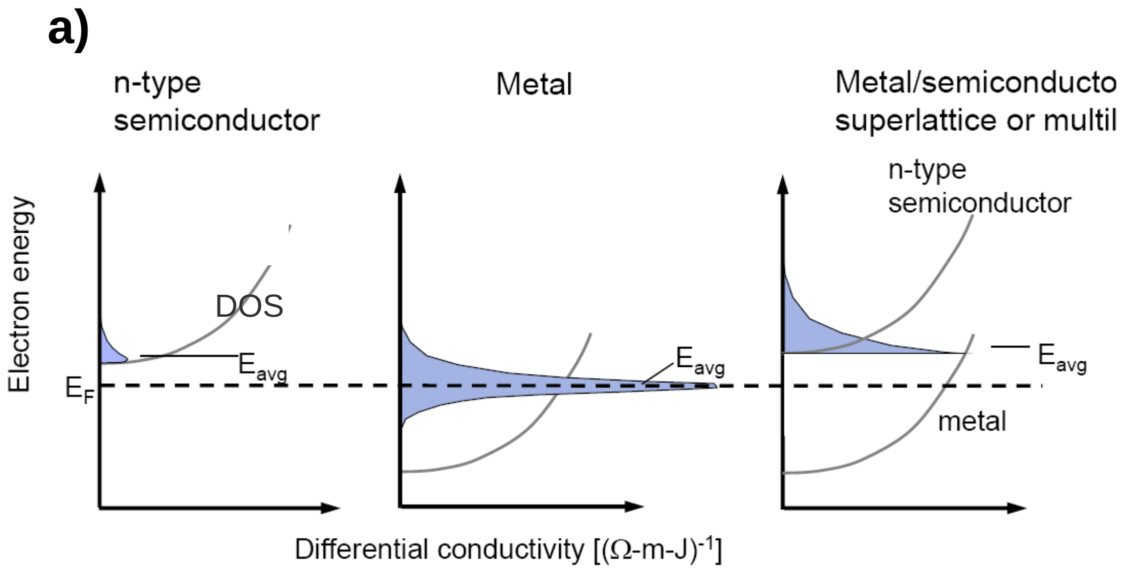

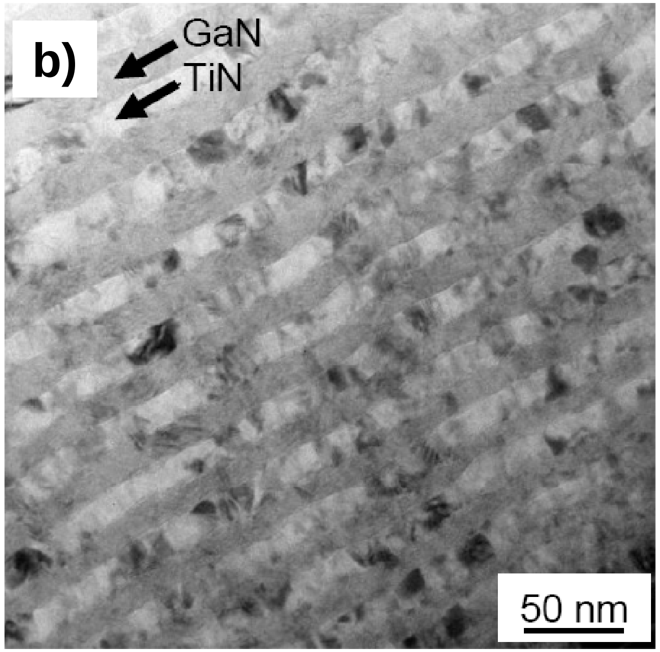

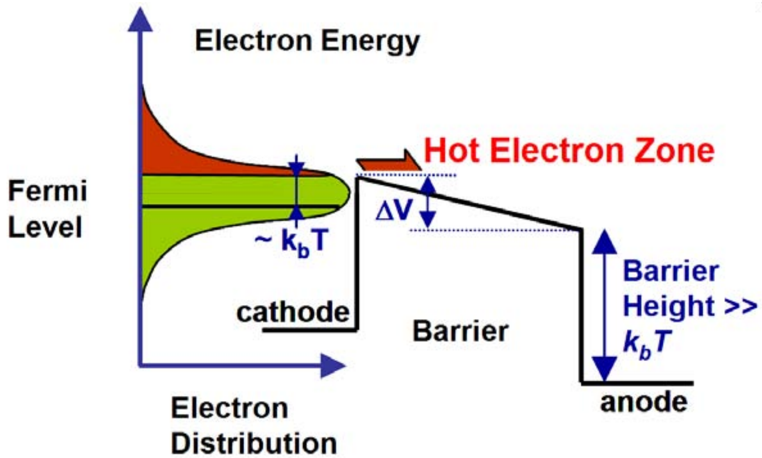

V. Rawat, T. Sands, J. Appl. Phys. 100 , 064901 (2006)

Synthesis of Nanograined Bulk-Materials

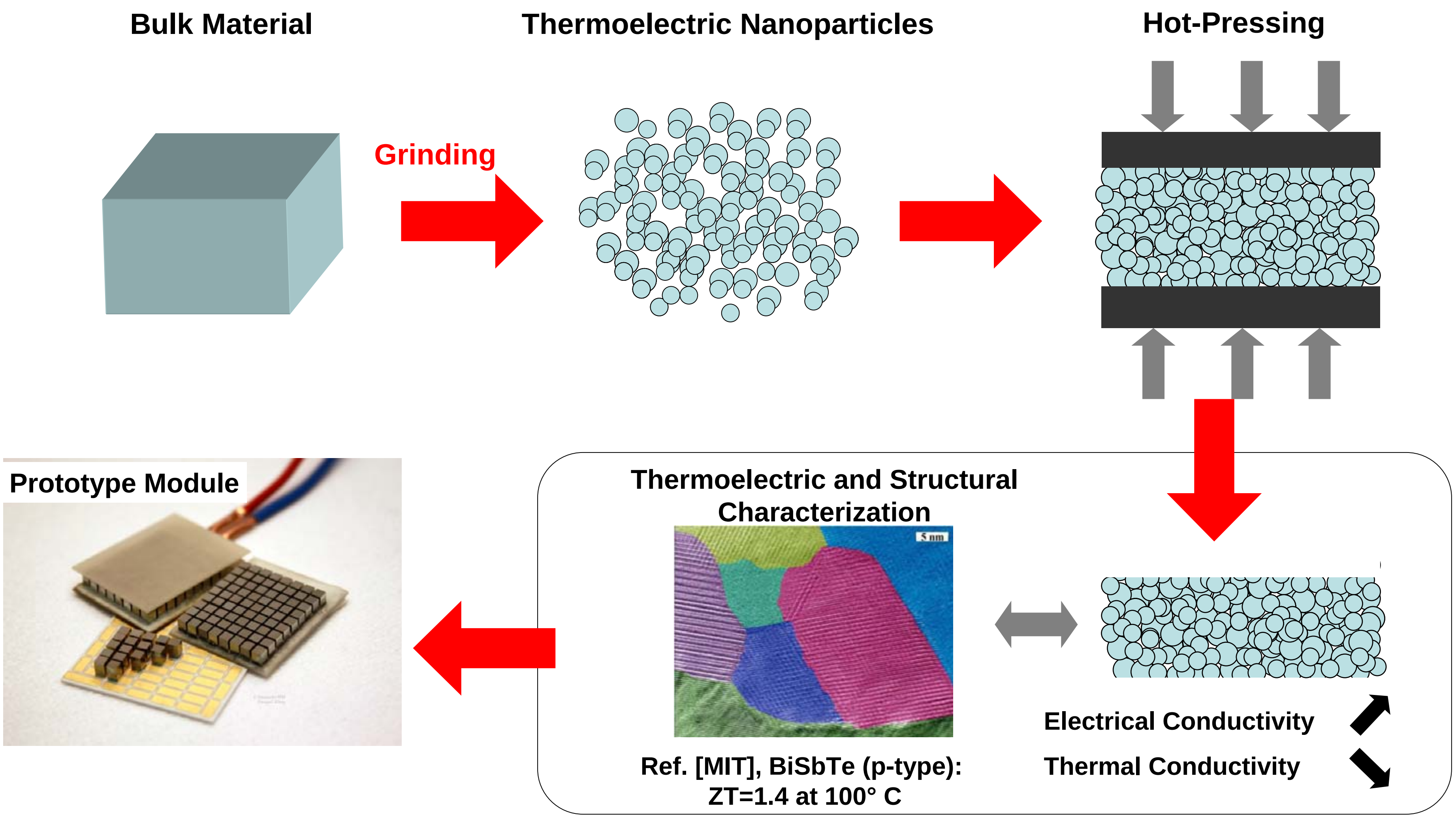

p-type (Sb/Bi)$_2$Te$_3$: Nanograined Bulk Materials

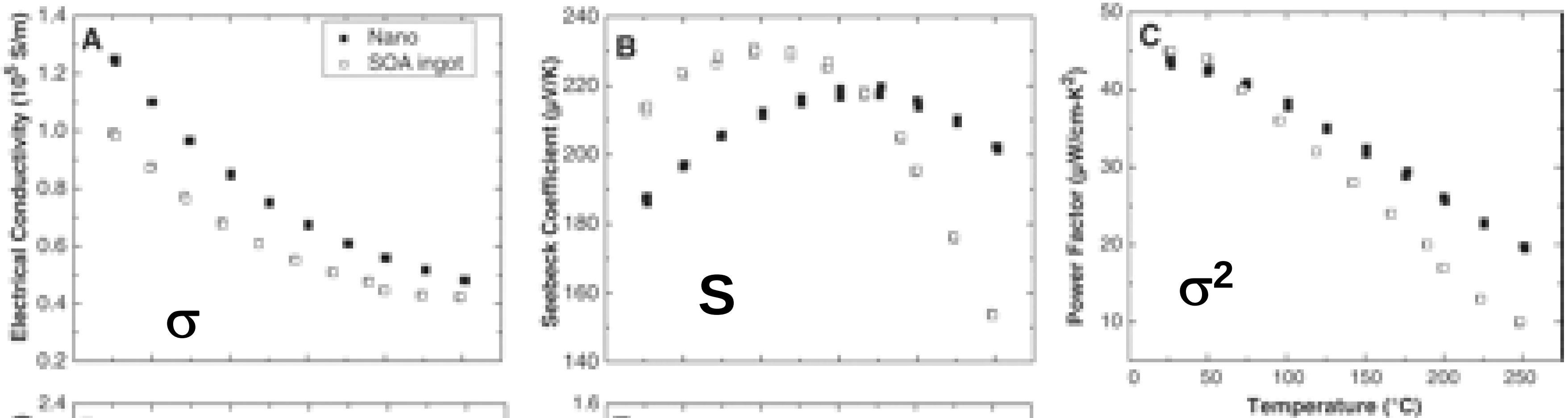

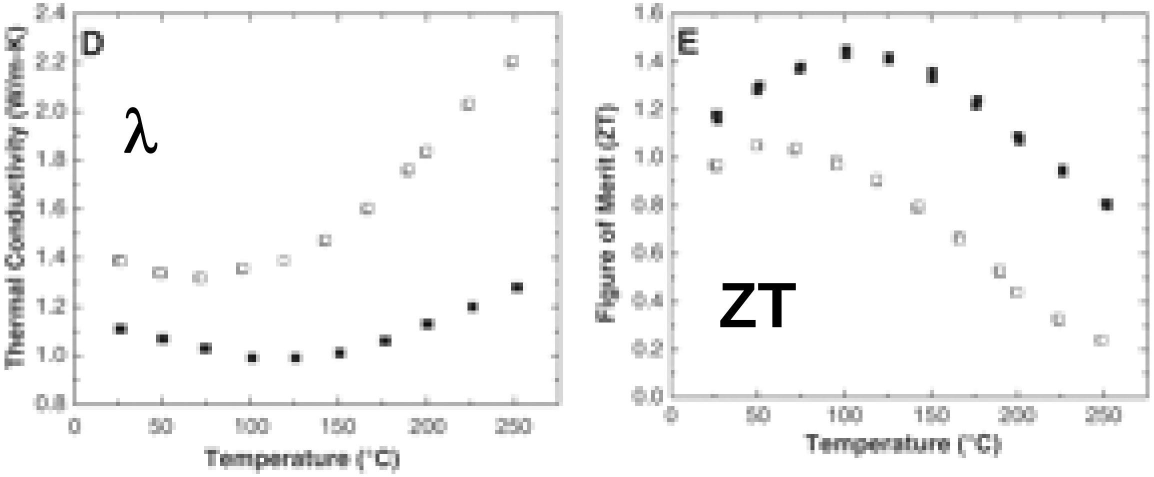

B. Poudel, Q. Hao, Y. Ma, Y. Lan, A. Minnich, B. Yu, Bo, X. Yan, D.Z. Wang, A. Muto, D. Vashaee, X.Y. Chen, JM. Liu, M.S. Dresselhaus, C. Gang, Z. Ren,
Science **320**, 634-638 (2008).

Nanograined Materials

Nanograined Material	Seebeck Coefficient [μV/K]	Thermal Conductivity [W/(mK)]	ZT	Methods and Comments	Reference
Bi_2Te_3 (p-type)	235	0.6	1.35 at 27° C	MS + SPS	20
$(Sb/Bi)_2Te_3$ (p-type)	210	0.95	1.4 at 100° C	BM of ingots and MA + HP	21,22
$Bi_{0.52}Sb_{1,48}Te_3$ (p-type)	240	0.65	1.56 at 27° C	MS + SPS	24,25
$Bi_2Te_{2.7}Se_{0.3}$ (n-type)	-220	0.8	1.04 at 125° C	MA + 2x HP	N4
$GaSb_{10}Te_{16}$ (p-type)	135	1.0	0.98 at 210° C	BM of ingots + SPS	N12
$AgSbTe_2$ (p-type)	200-200	0.39	0.99 at 400° C	MA + SPS	N10
PbTe (p-type)	320	1.0	0.4 at 100° C	BM + SPS	N1
PbTe:Tl (2%) (p-type)	330	1.0	1.5 at 500° C	Ingot synthesis	N2
PbTe:Tl (2%) (p-type)	295	0.95	1.3 at 400° C	BM + HP	N3
$(Pb_{0.95}Sn_{0.05}Te)_{0.92}(PbS)_{0.08}$ (n-type)	-260	1.0	1.5 at 380° C	Ingot synthesis	N7
$(PbTe)_{0.98}(SrTe)_{0.02}$ (p-type)	-300	0.9	1.7 at 530° C	Ingot synthesis	N8
$AgPb_{18}SbTe_{20}$ (p-type)	-380	0.95	2.1 at 530° C	Ingot synthesis	N11
$Ag_{0.8}Pb_{22}SbTe_{20}$ (p-type)	300	1.35 at RT	1.37 at 400° C	MA + SPS	N9
$Co_{0.8}Ni_{0.2}Sb_{3.05}$ (n-type)	-175	3	0.7 at 500° C	BM + SPS	45
$Yb_{0.2}Co_4Sb_{12.3}$ (n-type)	-200	2.2	1.26 at 530° C	MS + SPS	43
$Yb_{0.35}Co_4Sb_{12.3}$ (n-type)	-190	2.6	1.2 at 550° C	BM + SPS	44
$Mg_2Si_{0.6}Sn_{0.4}$:Sb (n-type)	-250	1.8	1.11 at 590° C	(BM of ingots + SPS) x 2	42
$Zr_{0.5}Hf_{0.5}CoSb_{0.8}Sn_{0.2}$ (p-type)	210	2.3	0.8 at 700° C	BM + SPS	46
$Si_{80}Ge_{20}$ (p-type)	260	2.3	0.95 at 900° C	BM + HP	36
$Si_{80}Ge_{20}$ (n-type)	-330	1.8	0.8 at 800° C	NPS by gas phase + SPS	N5
$Si_{80}Ge_{20}$ (n-type)	-280	1.8	1.3 at 900° C	BM + HP	35
$Si_{95}Ge_5$ (n-type)	-230	3	0.95 at 900° C	BM + HP	37
Si (n-type)	-200	4	0.7 at 900° C	BM + HP	38

Abbreviations: **BM** - Ball Milling; **HP** - Hot Pressing; **MA** - Mechanical Alloying; **MS** - Melt Spinning; **NPS** - Nanoparticle Synthesis from gas phase;
SPS - Spark Plasma Sintering;

German Priority Program SPP 1386 on Nanostructured Thermoelectrics

Mai 2007 Overview Publication in Physik Journal
Sep 2007 Planning Meeting in
Nov. 15 Submission for the Founding Proposal

Apr. 2008 Positive Announcement about SPP 1386
Jul 2008 Network Meeting in Hamburg (80 Part.)
Sep. 22 Submission of 35 Proposal

Dec 2008 Selection of the Project

Apr. 2009 Start of the individual Projects (18)

2009 to 2012 First Funding Period
2012 to 2015 Second Funding Period

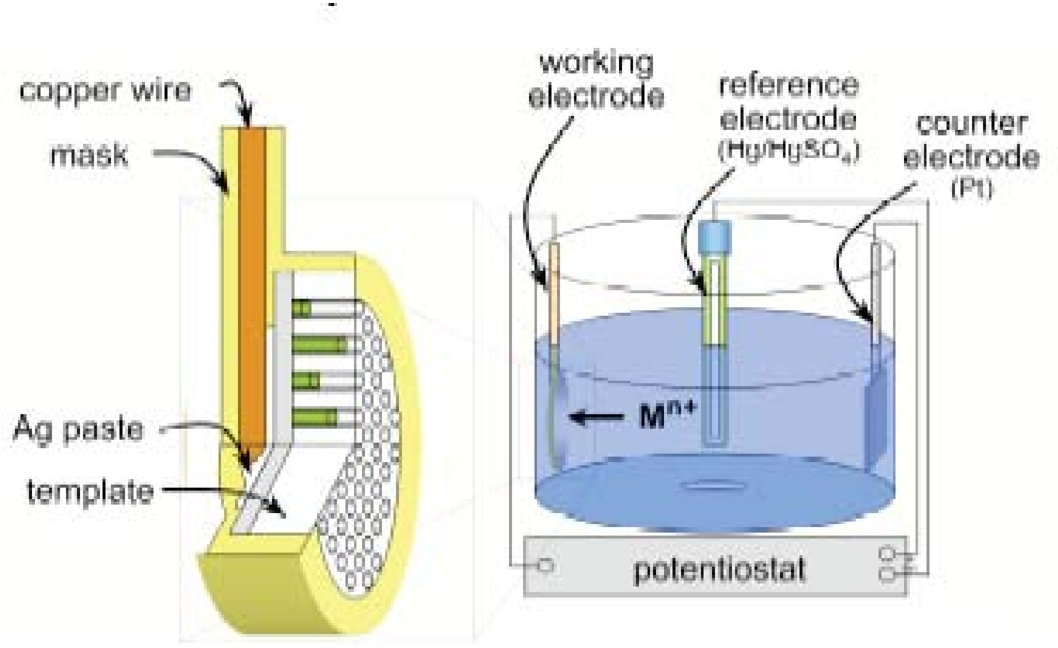
copper wire
mask
Ag paste
template
working electrode
reference electrode (Hg/HgSO4)
counter electrode (Pt)
M n+
potentiostat

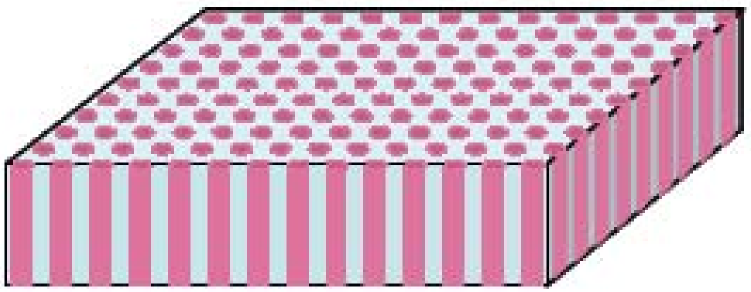

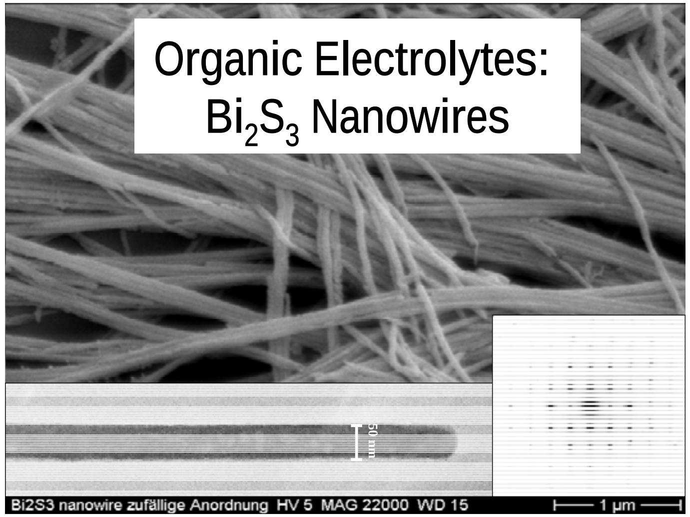
Organic Electrolytes:
Bi2S3 Nanowires
Bi2S3 nanowire zufällige Anordnung HV 5 MAG 22000 WD 15
1 µm

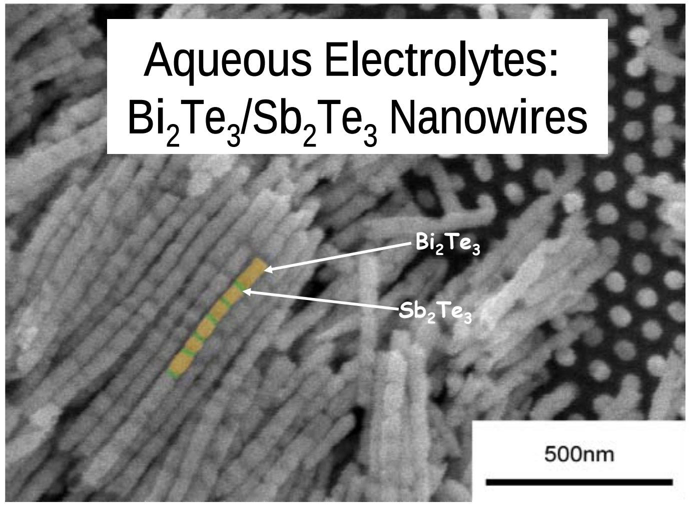
Aqueous Electrolytes:
Bi2Te3/Sb2Te3 Nanowires
Bi2Te3
Sb2Te3
500nm

Preparation procedure for the TE measurement:

Electrical conductivity of individual nanowires

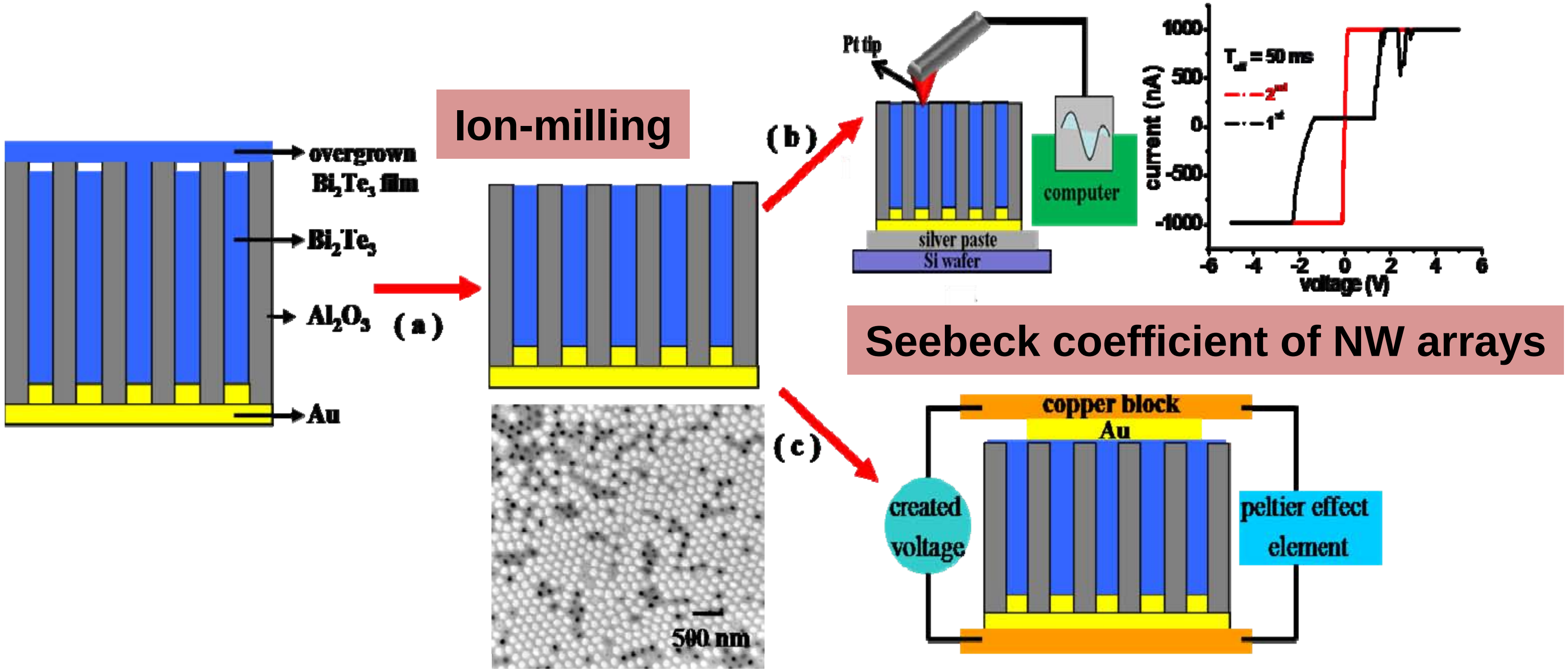

J.M. Lee, PSS-RRL in press DOI: 10.1002/pssr.200903368

Measurements of the Power Factor ($S^2\sigma$) for Bi_2Te_3 NWs

Representative linear *I-V* characteristic of an individual nanowire (T_{off} = 50 ms)

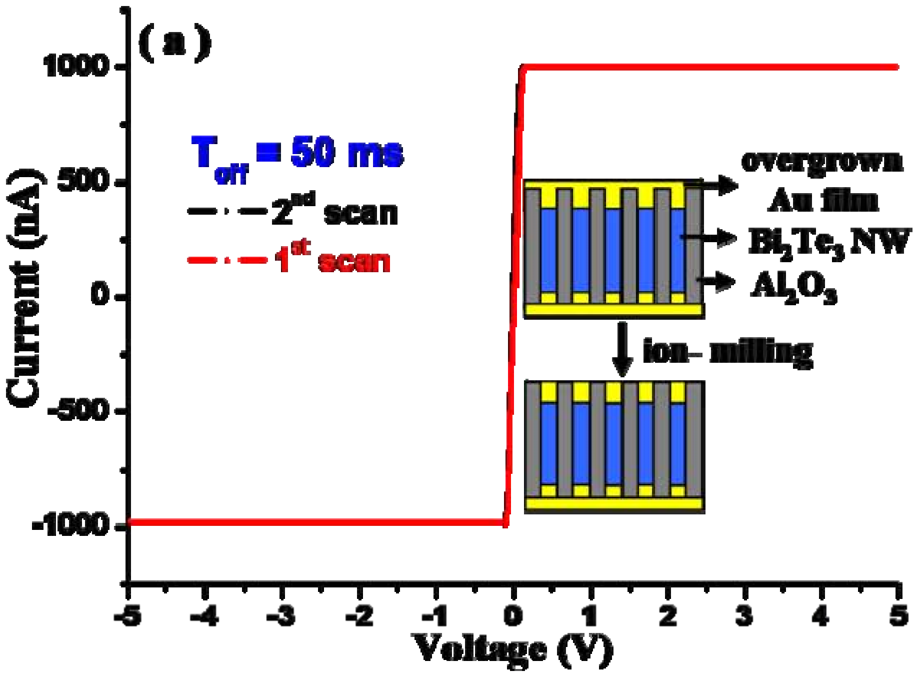

Cross-sectional SEM image of nanowires with off time of 20 ms

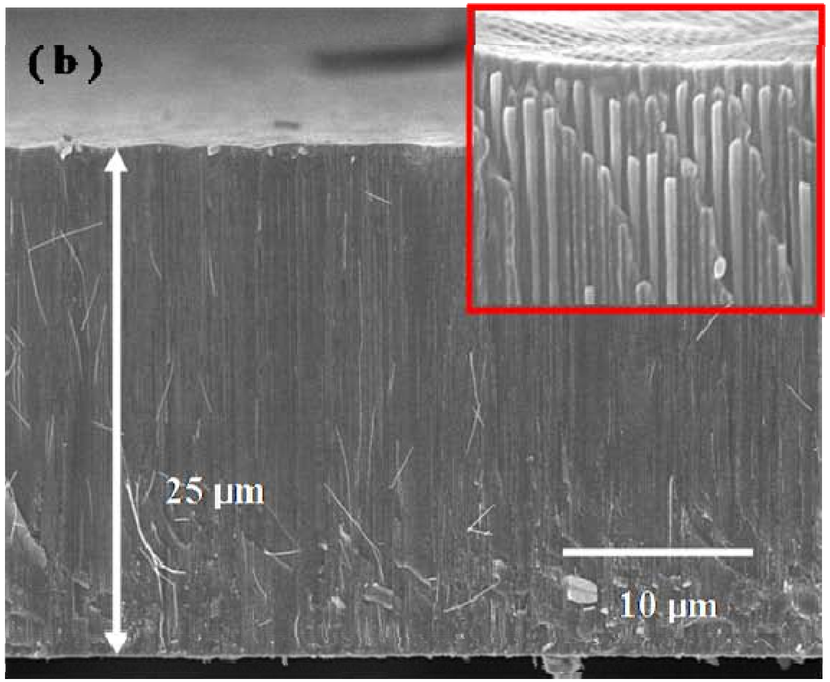

J.M. Lee, PSS-RRL 4, 43 (2010)

Measurements of the Power Factor ($S^2\sigma$) for Bi_2Te_3 NWs

Seebeck coefficient and atomic ratio (Te/ Bi)

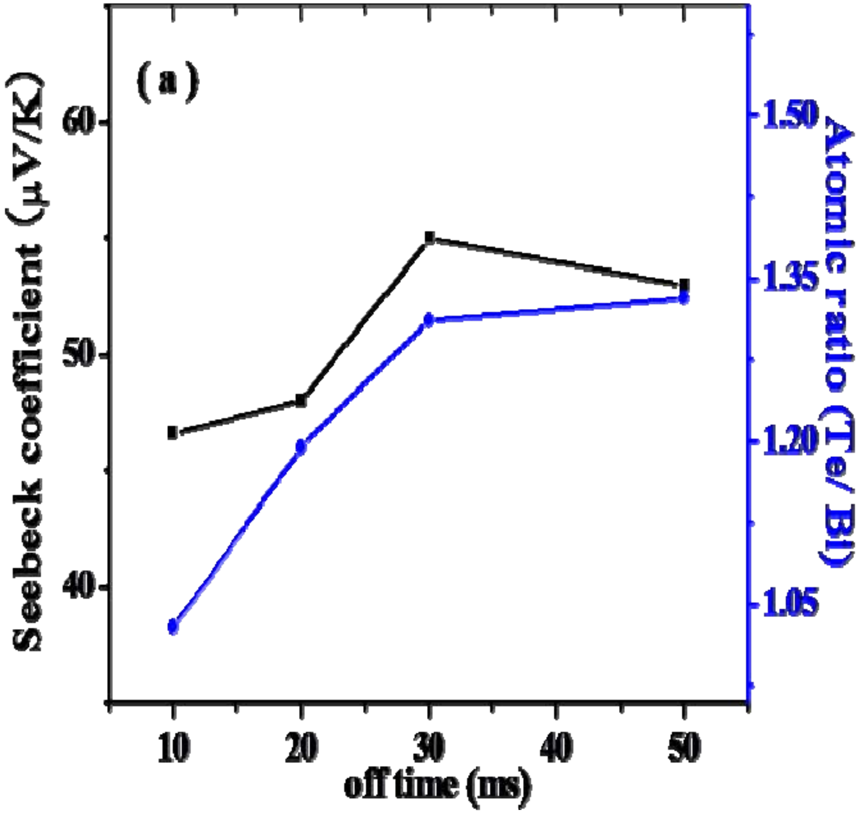

Power factor and electrical conductivity

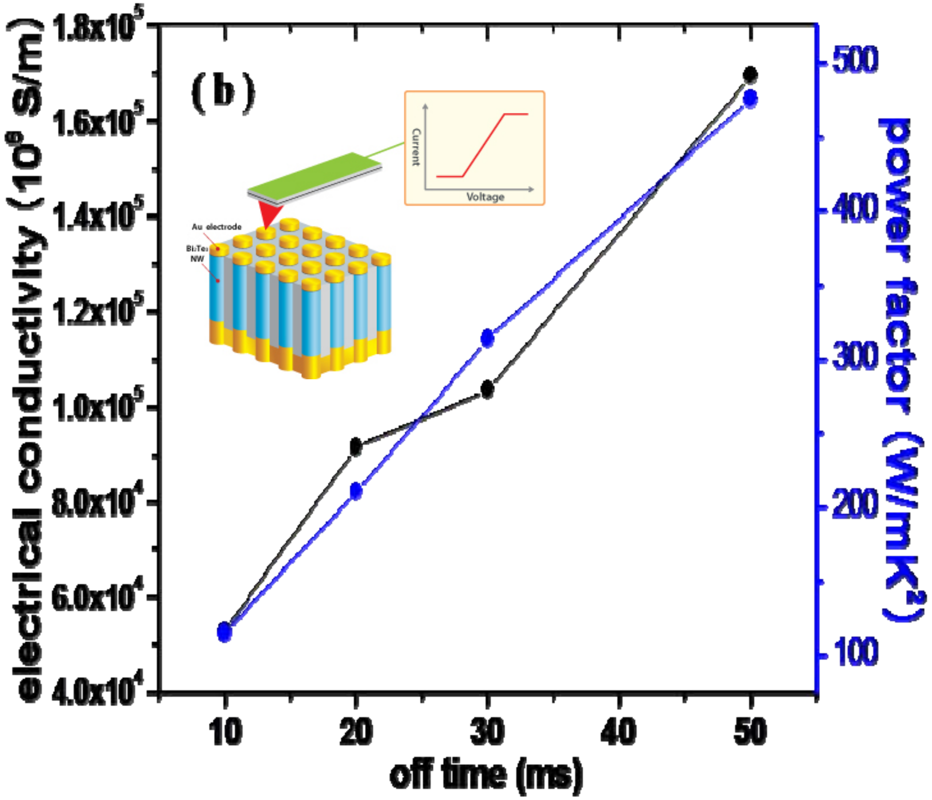

J.M. Lee, PSS-RRL 4, 43 (2010)

Single-Crystalline Bi_xTe_y-Nanowires close to Stochimetry

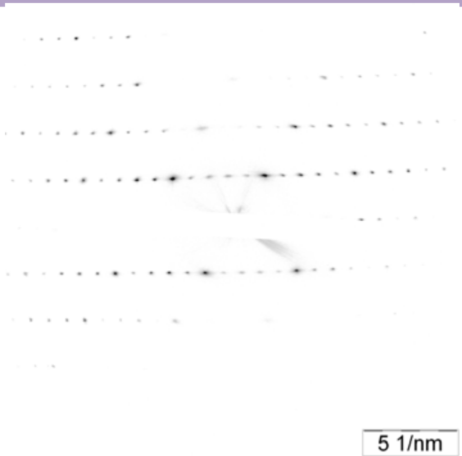

diffraction pattern of single nanowire

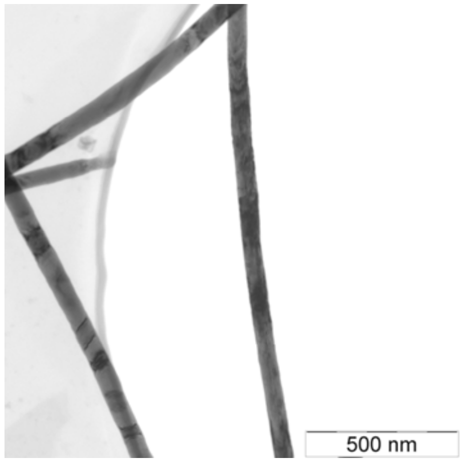

bright-field image

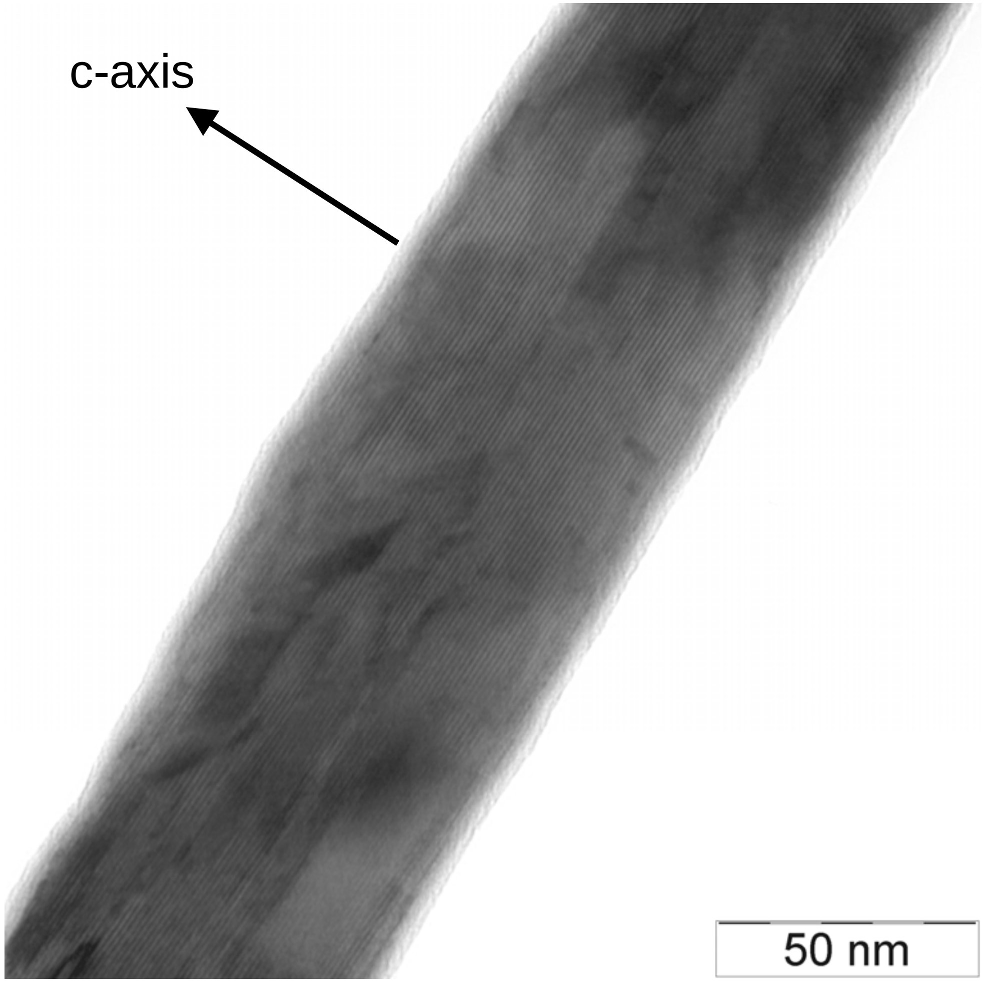

High Resolution TEM

Growth Directions of the Nanowires

Sb_2Se_3 wires *always* grow along the ***c*** axis;
Sb_2S_3 wires *preferentially* along ***b***:

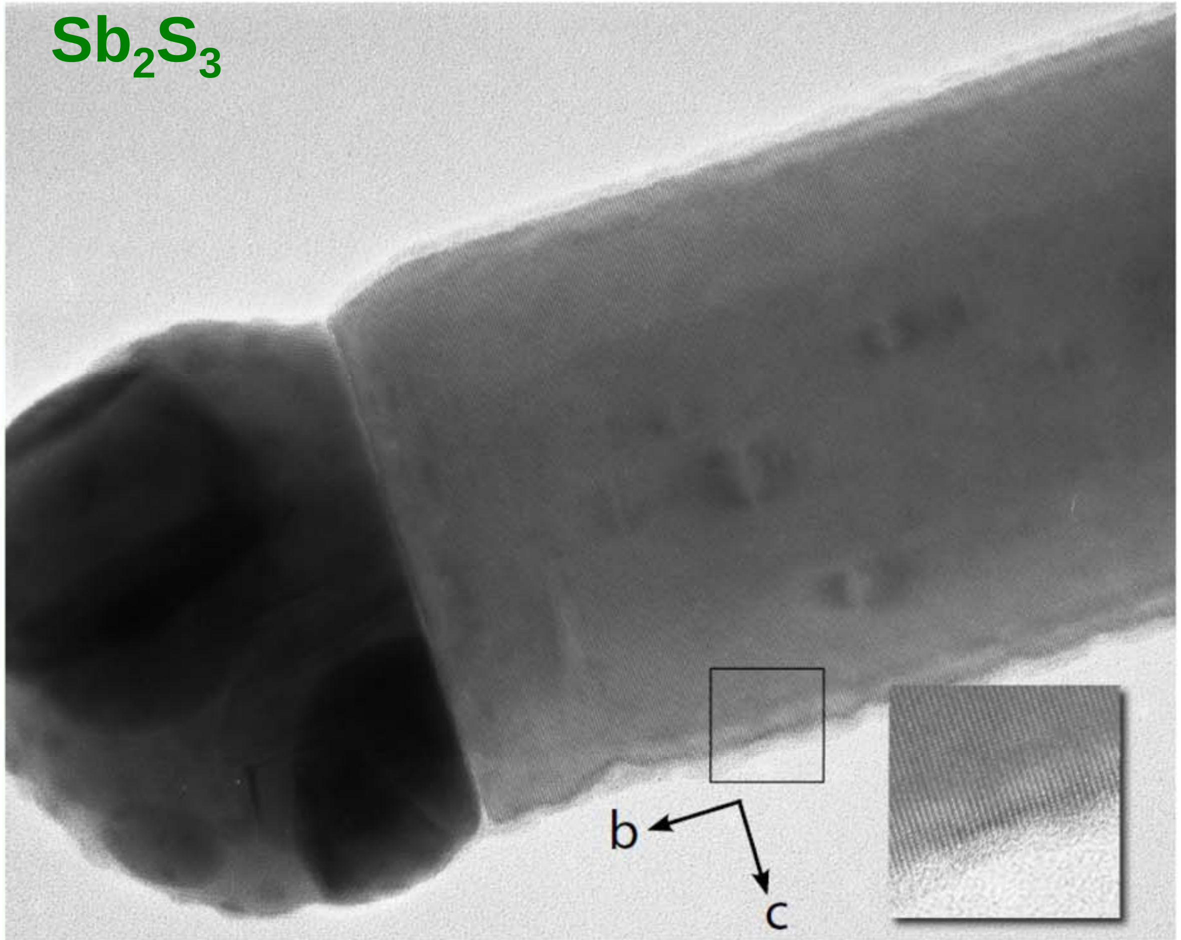

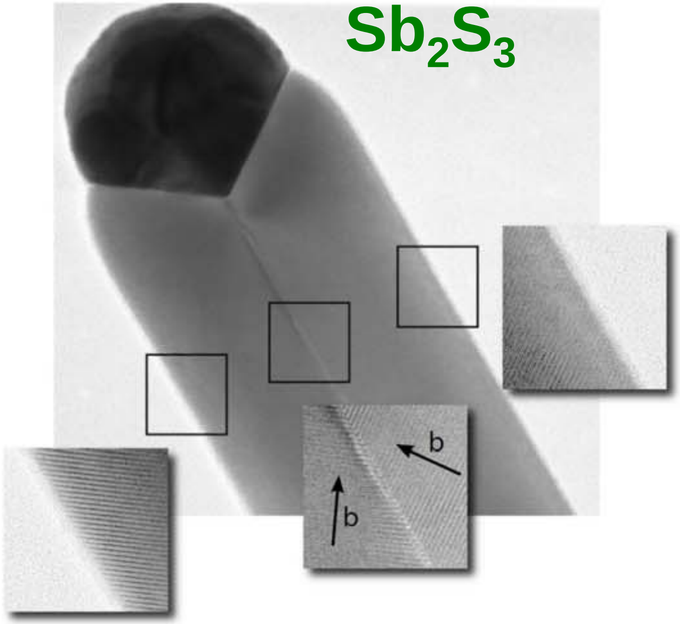

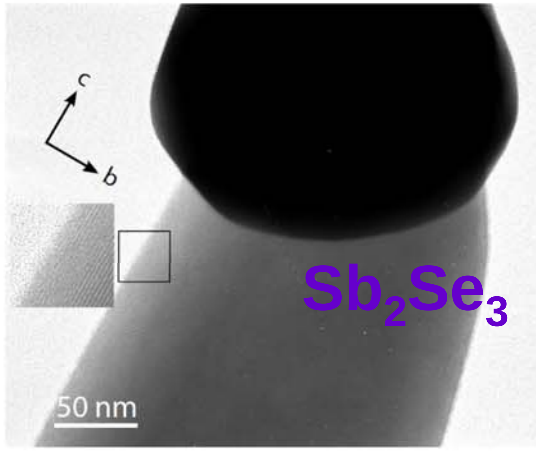

Atomic Layer Deposition (ALD) and Pulsed Vapor-liquid-solid (VLS) Growth

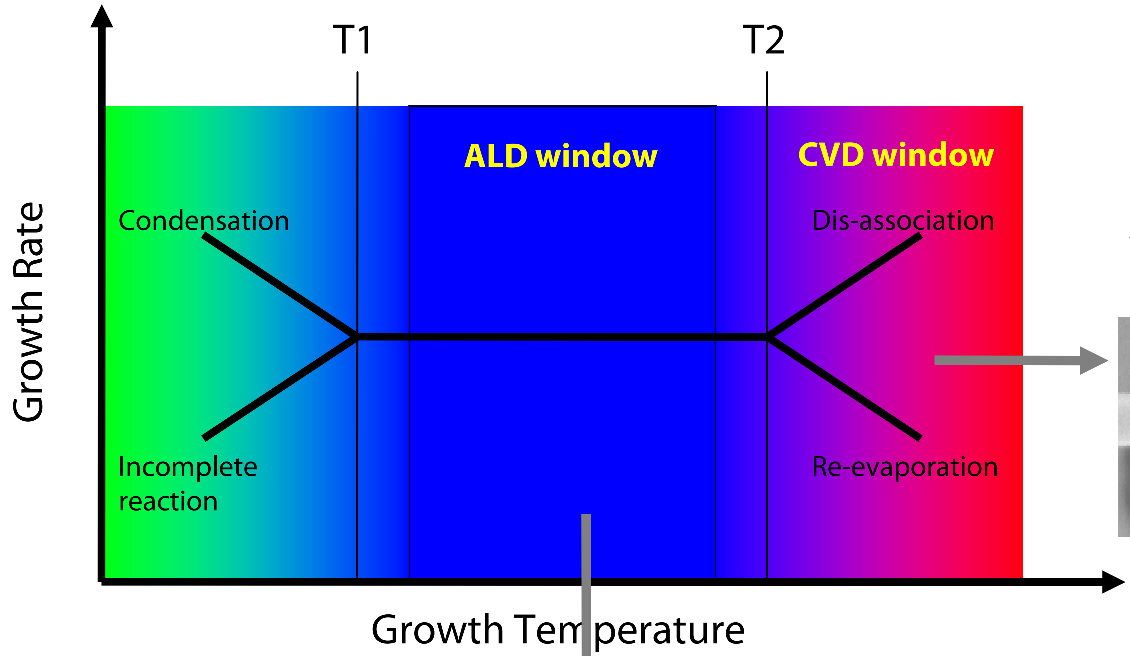

VLS growth via pulsed CVD. Single crystalline.

Films and nanotubes via ALD. Amorphous.

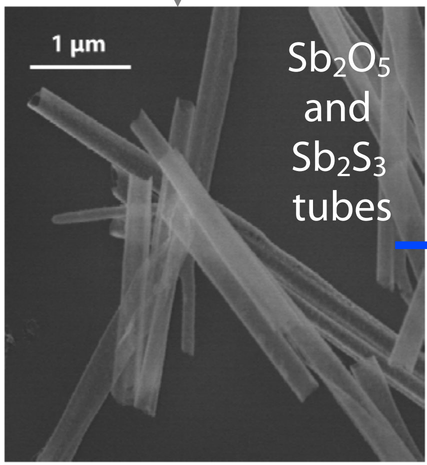

Epitaxial growth

Orthorhombic, Pbnm, highly anisotropic

	a[Å]	*b*[Å]	*c*[Å]
Sb_2S_3	11.299	11.310	3.839
Sb_2Se_3	11.620	11.770	3.962
Bi_2S_3	11.150	11.300	3.981

Sb_2Se_3 VLS + Sb_2S_3 ALD

ALD at 90°C: **core-shell structure**.

Shell is **crystalline** !

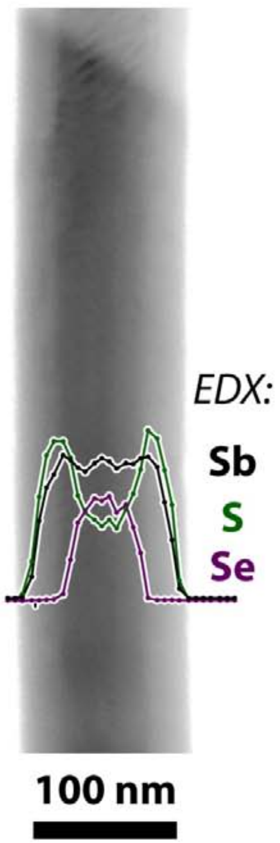

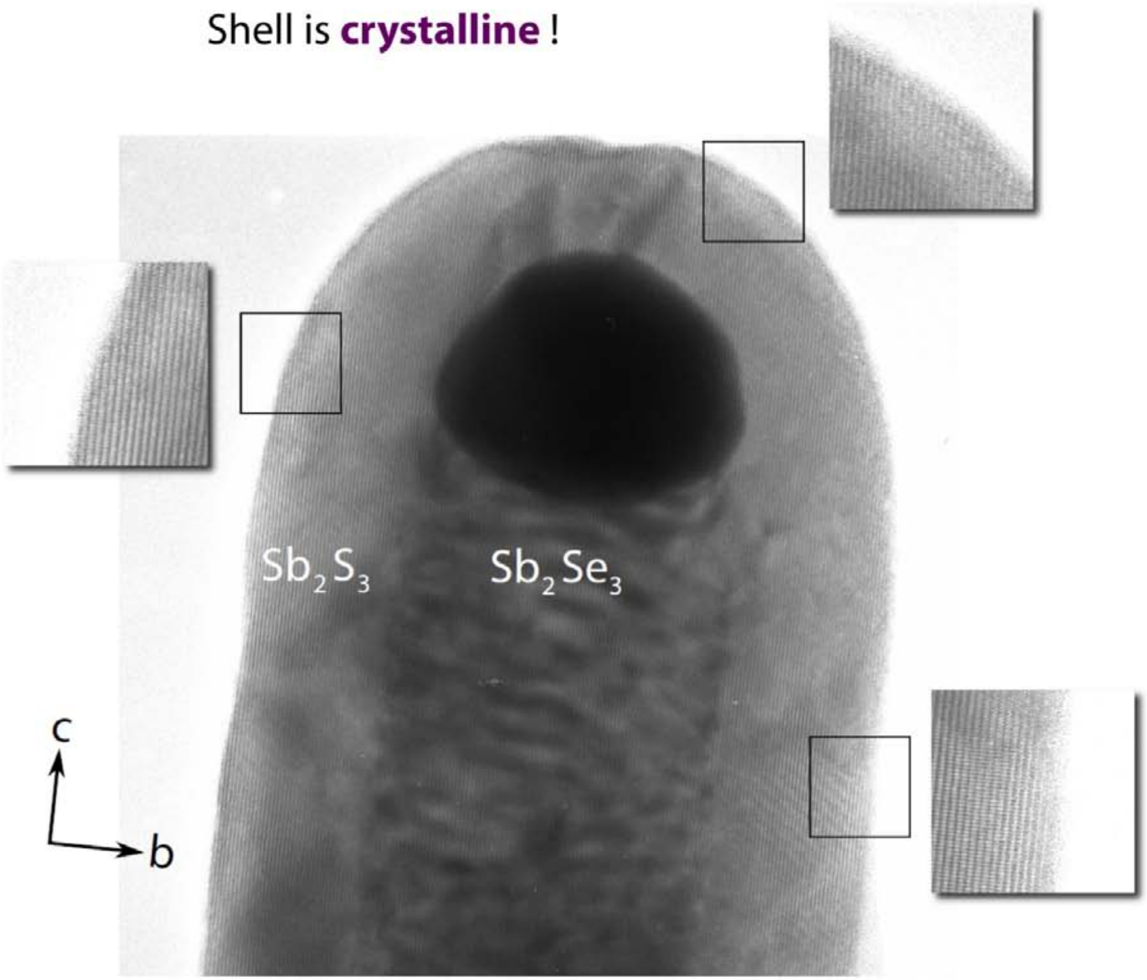

Concept of the 3-Omega Method

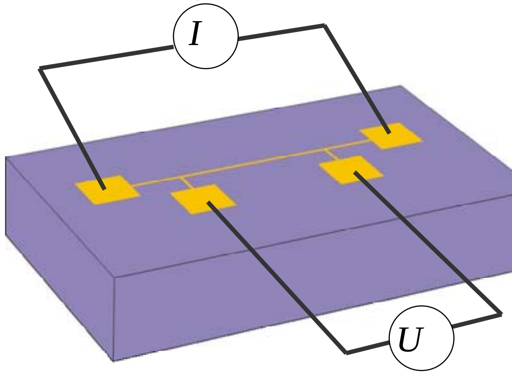

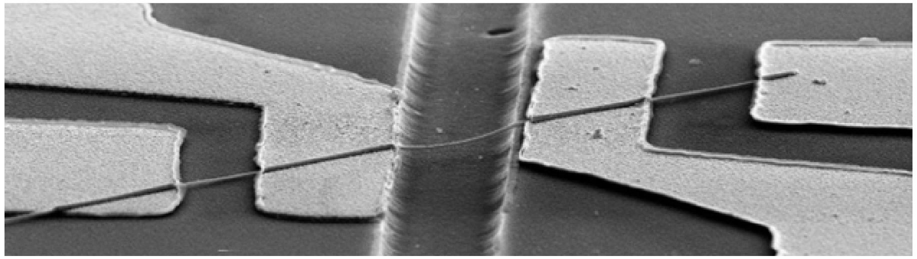

$$V_{3\omega}(t) \approx -\frac{2 I_0^3 L R R'}{\pi^4 \kappa S \sqrt{1+(2\omega\gamma)^2}} \sin(3\omega t - \phi)$$

[1]Rev. Sci. Instrum., Vol. 72, No. 7, July 2001

Thermal Conductivity

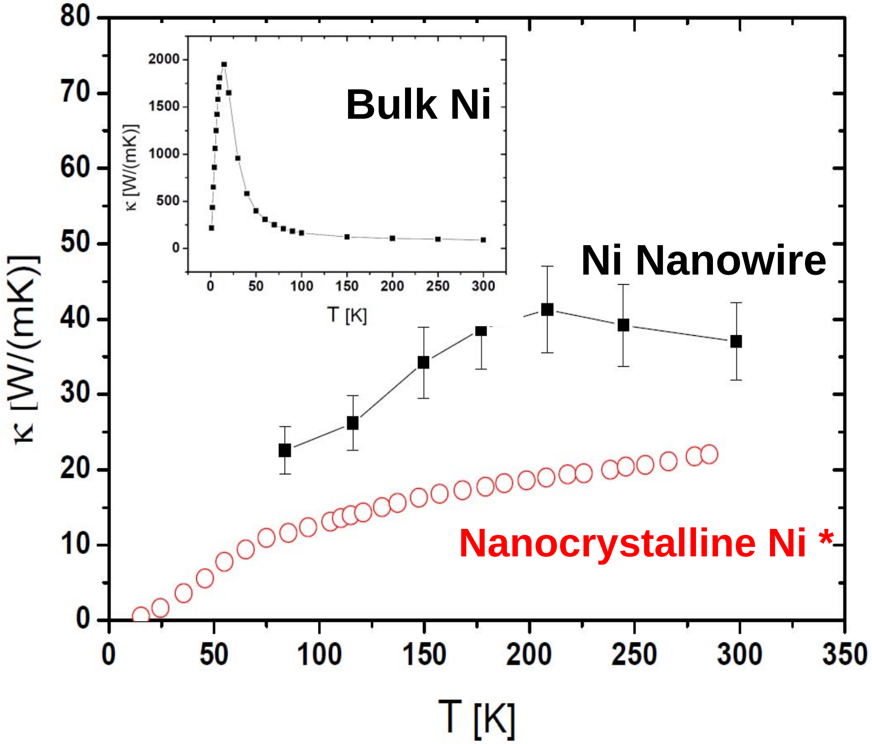

L length of the suspended wire

R' resistance change with temperature

S cross-section of the wire

γ thermal time constant

J. Kimling

Outlook: AMR in $Co_{50}Ni_{50}$ Nanowires

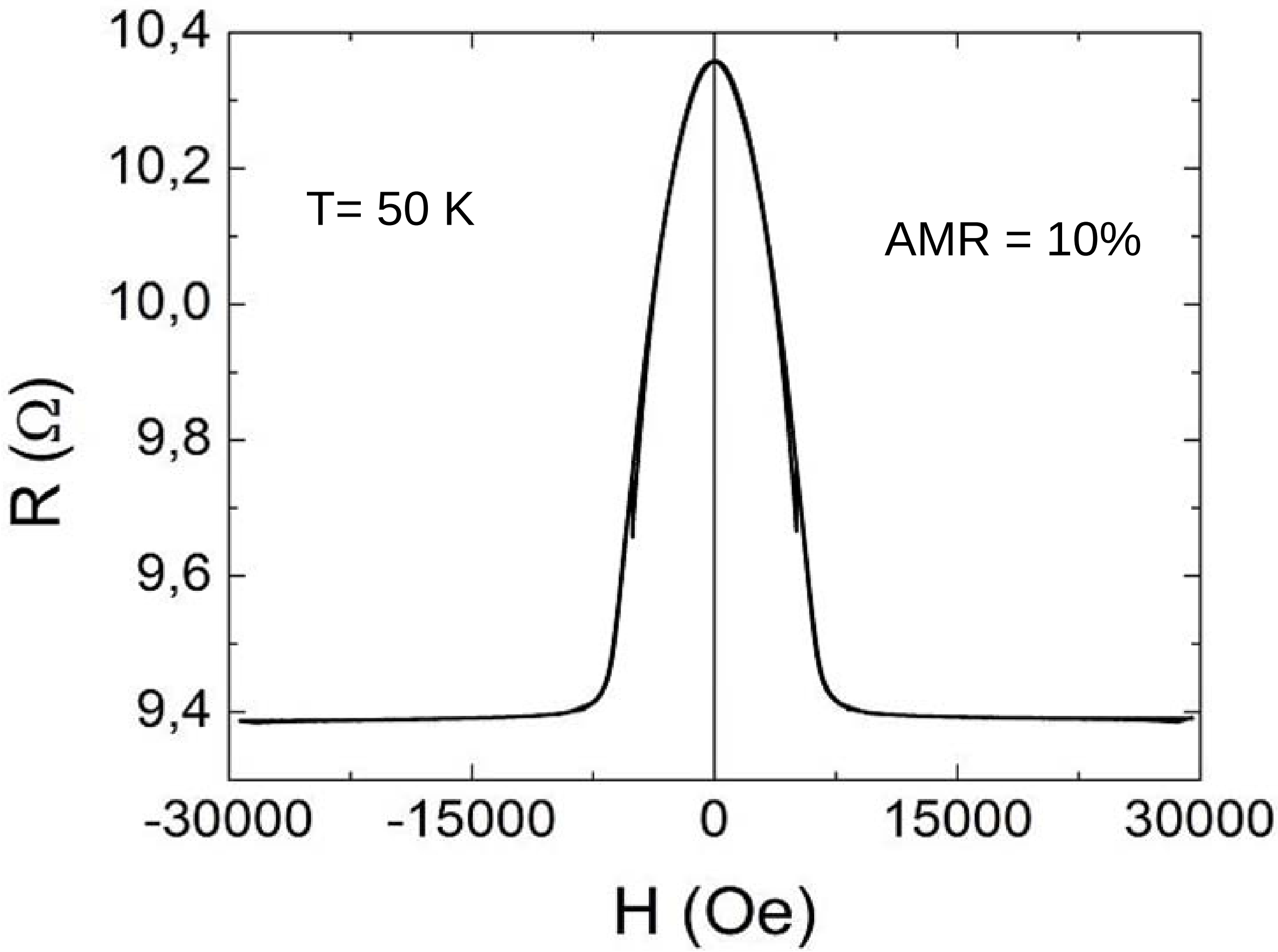

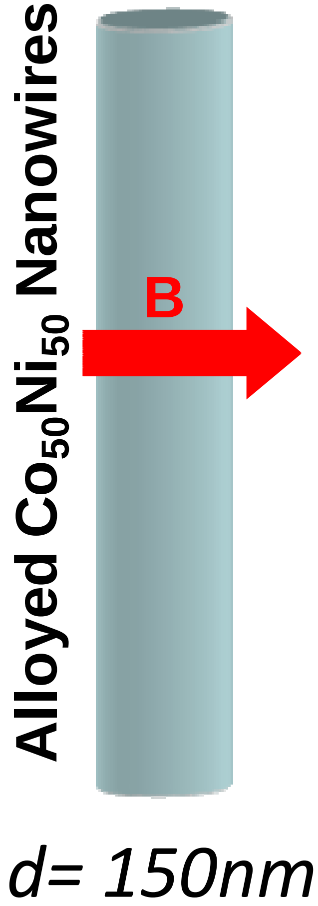

Nielsch Reiss Ansermet
Cross-Plane SpinCaT in Magnetoresistive Nanostructures

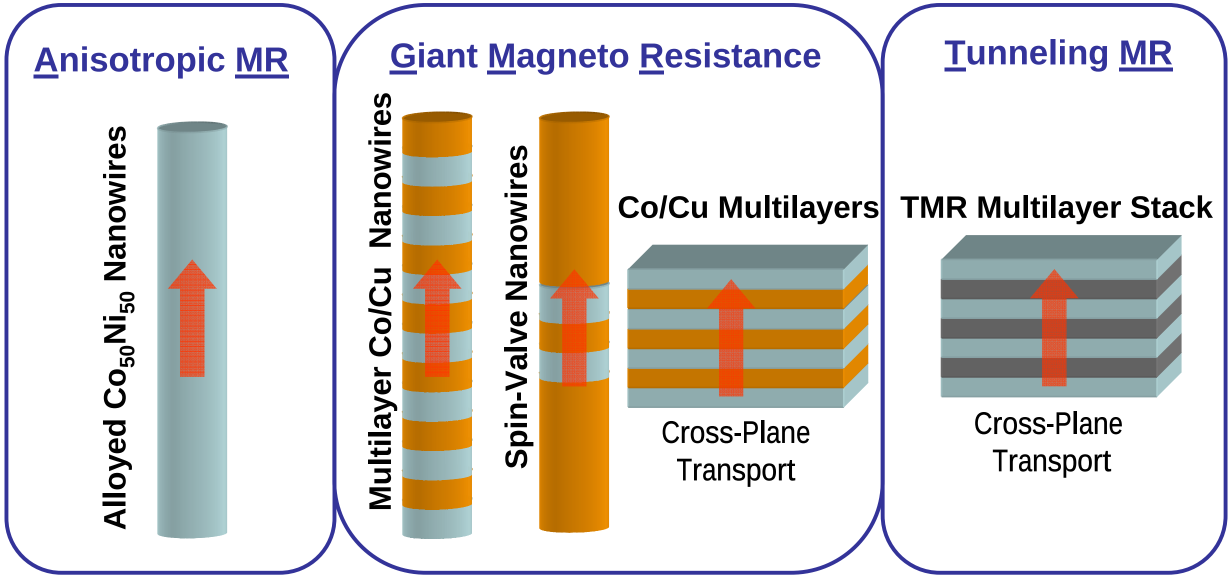

The major scientific questions:

- Spin-dependent thermal conductivity
- Lorenz Number and Wiedemann Franz Law in NWs
- Absolute Seebeck coefficient and magneto-thermoelectric conversation efficiency in NWs: ZT (B)
- Detection of spin waves in NW under strong heat flow by FMR